Mixed layer depth over the global ocean: An examination of profile data and a profile-based climatology

Clément de Boyer Montégut, Gurvan Madec, Albert S. Fischer,[1] Alban Lazar, and Daniele Iudicone[2]

Laboratoire d'Océanographie Dynamique et de Climatologie, Institut Pierre Simon Laplace, Unité Mixte de Recherche, CNRS/IRD/UPMC, Paris, France

[1] A new 2° resolution global climatology of the mixed layer depth (MLD) based on individual profiles is constructed. Previous global climatologies have been based on temperature or density-gridded climatologies. The criterion selected is a threshold value of temperature or density from a near-surface value at 10 m depth ($\Delta T = 0.2$°C or $\Delta\sigma_\theta = 0.03$ kg m^{-3}). A validation of the temperature criterion on moored time series data shows that the method is successful at following the base of the mixed layer. In particular, the first spring restratification is better captured than with a more commonly used larger criteria. In addition, we show that for a given 0.2°C criterion, the MLD estimated from averaged profiles results in a shallow bias of 25% compared to the MLD estimated from individual profiles. A new global seasonal estimation of barrier layer thickness is also provided. An interesting result is the prevalence in mid- and high-latitude winter hemispheres of vertically density-compensated layers, creating an isopycnal but not mixed layer. Consequently, we propose an optimal estimate of MLD based on both temperature and density data. An independent validation of the maximum annual MLD with oxygen data shows that this oxygen estimate may be biased in regions of Ekman pumping or strong biological activity. Significant differences are shown compared to previous climatologies. The timing of the seasonal cycle of the mixed layer is shifted earlier in the year, and the maximum MLD captures finer structures and is shallower. These results are discussed in light of the different approaches and the choice of criterion.   *INDEX TERMS:* 4572 Oceanography: Physical: Upper ocean processes; 4568 Oceanography: Physical: Turbulence, diffusion, and mixing processes; 4227 Oceanography: General: Diurnal, seasonal, and annual cycles; *KEYWORDS:* mixed layer, mixed layer depth criterion, density compensation

1. Introduction

[2] A striking and nearly universal feature of the open ocean is the surface mixed layer within which salinity, temperature, and density are almost vertically uniform. This oceanic mixed layer is the manifestation of the vigorous turbulent mixing processes which are active in the upper ocean. The transfer of mass, momentum, and energy across the mixed layer provides the source of almost all oceanic motions, and the thickness of the mixed layer determines the heat content and mechanical inertia of the layer that directly interacts with the atmosphere.

[3] The main temporal variabilities of the MLD are directly linked to the many processes occurring in the mixed layer (surface forcing, lateral advection, internal waves, etc), ranging from diurnal [*Brainerd and Gregg*, 1995] to interannual variability, including seasonal and intraseasonal variability [e.g., *Kara et al.*, 2003a; *McCreary et al.*, 2001]. The spatial variability of the MLD is also very large. The MLD can be less than 20 m in the summer hemisphere, while reaching more than 500 m in the winter hemisphere in subpolar latitudes [*Monterey and Levitus*, 1997]. Therefore many different features in surface layer profiles may occur in the global ocean [*Sprintall and Roemmich*, 1999].

[4] Despite these difficulties in properly defining the MLD, compounded by the lack of temperature and salinity data in some regions of the global ocean, a MLD climatology is necessary and essential in understanding the climatic system. Indeed, such a climatology is of primary importance for ocean modelers in validating and improving mixed layer

---

[1] Now at Intergovernmental Oceanographic Commission, UNESCO, Paris, France.
[2] Now at Laboratory of Biological Oceanography, Stazione Zoologica, Villa Comunale, Naples, Italy.

Table 1. Examples of Criteria Used to Define the So-Called MLD From a Threshold Method, for Which the MLD is the Depth at Which Temperature T or Potential Density σ_θ Change by a Given Threshold Value, ΔT or $\Delta\sigma_\theta$, Relative to the One at a Reference Depth $(Z_{ref})^a$

Author and Area Studied	Profiles	MLD Threshold Criterion	Z_{ref}	Criterion Choice
Sprintall and Roemmich [1999], Pacific Ocean	ind	$\Delta T = 0.1°C$ $\Delta\sigma_\theta = \frac{\partial\sigma_\theta}{\partial T}\Delta T$ with $\Delta T = 0.1°C$	10 m	direct observation of more than 1000 profiles
Kara et al. [2000b], Global Ocean	ave	$\Delta T = 0.8°C$ $\Delta\sigma_\theta = \sigma_\theta(T + \Delta T, S) - \sigma_\theta(T, S)$ with $\Delta T = 0.8°C$	10 m	statistical comparison with Ocean Weather Station data
Monterey and Levitus [1997], Global Ocean	ave	$\Delta T = 0.5°C$ $\Delta\sigma_\theta = 0.125$ kg m^{-3}	0 m	$\Delta\sigma_\theta$ corresponds to water mass characteristics of subtropical mode water in North Atlantic ΔT corresponds to $\Delta\sigma_\theta$ within 17 to 19°C and $S = 35$ *PSU*
Brainerd and Gregg [1995], Pacific Ocean	ind	$\Delta\sigma_\theta = 0.05$ to 0.5 kg m^{-3}	0 m	direct observation of overturning length
Suga et al. [2004], North Pacific	ind	$\Delta\sigma_\theta = 0.125$ kg m^{-3}	10 m	arbitrary
Thomson and Fine [2003], North Pacific	ind	$\Delta\sigma_\theta = 0.01$ to 0.03 kg m^{-3}	2.5 m	arbitrary
Weller and Plueddeman [1996], North Pacific	ind	$\Delta\sigma_\theta = 0.03$ kg m^{-3}	10 m	arbitrary
Schneider and Müller [1990], Tropical Pacific	ind	$\Delta\sigma_\theta = 0.01$ or 0.03 kg m^{-3}	2.5 m	corresponds to subjective estimate of MLD
Obata et al. [1996], Global Ocean	ave	$\Delta T = 0.5°C$	0 m	arbitrary
Thompson [1976], North Pacific	ind	$\Delta T = 0.2°C$	3 m	arbitrary
Spall et al. [2000], North Atlantic	ind	$\Delta T = 0.5°C$	0 m	arbitrary
Foltz et al. [2003], Tropical Atlantic	ind	$\Delta T = 0.5°C$	0 m	arbitrary
Rao et al. [1989], Indian Ocean	ind	$\Delta T = 1°C$	10 m	arbitrary

[a]The type of profiles investigated by the author is also mentioned, "ind" for individual and "ave" for monthly averaged profiles, and the way they choose their criterion.

parameterizations and Ocean General Circulation Models [e.g., *Chen et al.*, 1994; *Masson et al.*, 2002; *Noh et al.*, 2002; *Kara et al.*, 2003b; *Zhang and Zebiak*, 2002]. Information on barrier layer regions [*Kara et al.*, 2000a] and diagnostics of atmosphere and ocean trends in mixed layer budgets [e.g., *Rao and Sivakumar*, 2003; *Foltz et al.*, 2003] are other examples. In addition, as almost all biological activity is restricted to the upper ocean within the euphotic zone, a MLD climatology can also be very useful in biological studies [e.g., *Morel and Andre*, 1991; *Longhurst*, 1995; *Polovina et al.*, 1995].

[5] The concept of the mixed layer is arbitrary, and can be based on different parameters (e.g., temperature, density, salinity), and may represent averages over different time intervals (e.g., day, month). Table 1 gives an example of the diversity of criteria used to determine the MLD using the threshold method, for which the MLD is the depth at which temperature or potential density changes by a given threshold value relative to the one at a near-surface reference depth. Most often the choice of these two crucial values is rather arbitrary. However, *Sprintall and Roemmich* [1999] used a visual examination of thousands of profiles in choosing their criterion, and *Brainerd and Gregg* [1995] studied the oceanic mixed layer in great detail using the Advanced Microstructure Profiler, from which they could estimate the length scale of turbulent overturns and the dissipation rate of turbulent kinetic energy. In work by *Kara et al.* [2000b], the optimal criterion value of 0.8°C was deduced through statistical comparisons of ocean weather station observations with good long-term monthly time series with the Levitus climatology. Lastly, *Levitus* [1982] chose a value of 0.125 kg m^{-3} in density, as it corresponds to the water

mass characteristics of Subtropical Mode Water in the North Atlantic.

[6] Only a few previous studies have produced a global MLD climatology [*Levitus*, 1982; *Monterey and Levitus*, 1997; *Kara et al.*, 2003a] (the two latter hereinafter referred to as KRH03 and ML97). The latter two were based on the Levitus World Ocean Atlas of 1994, and their estimation was based on already averaged and interpolated profiles. Estimating the MLD from individual profiles is another way to proceed, and has already been used in regional studies, such as the Indian Ocean or North Pacific Ocean [*Rao et al.*, 1989; *Suga et al.*, 2004]. Fields of MLD from individual profiles have also been produced to study some local phenomena such as barrier layers in the western equatorial Pacific and Atlantic Oceans [*Sprintall and McPhaden*, 1994; *Pailler et al.*, 1999].

[7] Unlike the studies of ML97 or KRH03, we compute global climatological monthly MLD by processing observed individual profiles of temperature and salinity. The main goal of this work is to create a global climatology of the MLD from the latest data set available, in order to have more information about the variability of this crucial layer. The mixed layer we want to study is the seasonal one, recently mixed in the last day or more. This mixed layer should also be vertically homogeneous in all tracers (temperature, salinity, and density) as we are interested in it from a thermodynamical point of view, as the receptacle of air-sea fluxes. We also use oxygen data to evaluate a proxy of the maximum depth reached by the oceanic mixed layer every year, the so-called "bowl" [*Guilyardi et al.*, 2001]. Because averaging and interpolating temperature or salinity results in a smoothed profile

and can even create artificial mixing of water masses, we determine MLD from individual profiles, capturing every temporal fluctuation linked to the processes of this layer.

[8] The data sources and methodology are presented in section 2. Then in section 3, we investigate the mixed layer physics to choose the best criterion to estimate the MLD. In section 4, we present a global overview of the temperature-based MLD climatology, followed by a discussion of our method. We also investigate the impact of salinity on MLD with barrier layers and compensated layers. Section 5 is a study of the characteristics of the maximum MLD in comparison with other climatologies in the North Atlantic, or with estimations based on oxygen data on a global scale. Section 6 is the summary and conclusion of this work.

2. Data Sources and Methodology

2.1. Data Sources and Distribution

[9] The 4,490,571 original hydrographic profiles used in this study were obtained from the National Oceanographic Data Center [*Conkright et al.*, 2002] and from the World Ocean Circulation Experiment database [*WOCE Data Products Committee*, 2002]. They represent all the high vertical resolution data available since 1941 through 2002, including Mechanical BathyThermograph (MBT), eXpendable BathyThermograph (XBT), Conductivity-Temperature-Depth (CTD), and Profiling FLoats (PFL).

[10] The seasonal spatial distributions of the data used in this analysis are shown in Figure 1, with the most striking feature being the difference in coverage between south and north. This difference exists for temperature but is even stronger for salinity, with a real lack of data in the Southern Ocean, not only in austral winter but in spring and autumn as well, while the tropical and northern Atlantic Ocean are almost completely covered in each season. The seasonal distribution of temperature data is extensive in the Northern Hemisphere and is reasonable in the Southern Hemisphere, with about 10 profiles per grid box north of 50°S, but data are still quite sparse south of that limit, especially in winter. Figure 2 shows the temporal distribution of the data. The number of profiles per year increases from 1941 to 1960, reaching 80,000 per year or more through the 1990s. Then the decrease in available data is obviously the consequence of an accumulated lag between data collection, submission to NODC, and data entry into the archives.

2.2. Methodology

[11] A detailed description of the steps followed to produce MLD climatologies from individual profiles can be found in Appendix A. We first select profiles without any spurious data in the mixed layer. This removes about 8% of the total profiles. For each of the selected profiles, we estimate a MLD following the chosen criterion (see section 3), and we gather these values into monthly boxes of 2° latitude by 2° longitude.

[12] The reduction of the data is a delicate step, as we must find the most appropriate estimator that best characterizes the ensemble of MLDs for each grid box. Here the distributions of these MLDs are most often skewed toward higher values (for example, see April in Figure 3 for the $\Delta T = 0.2°C$ criterion). Therefore the median is a more robust estimator than the mean of the MLDs. One must keep in mind that this reduction, though necessary, is fairly severe, as each grid box contains all the time variability of the mixed layer, which can lead to a great range of MLDs and broad distributions. This is most marked during the spring restratification, as wintertime deep mixed layers are replaced by thin restratified mixed layers, often creating a bimodal distribution that reflects both intramonthly and interannual variability (more in section 3.2).

[13] The next step consisted of a slight smoothing to take into account the noisy nature of ship observations [*Terray*, 1994]. Finally, ordinary kriging was used as the optimal prediction method to fill in missing grid point values. This prediction was limited to a 1000-km radius disk containing at least 5 grid point values, leaving some regions without value rather than filled by a doubtful interpolation. The advantage of kriging is that it is an exact interpolator, and an estimation error in the form of the kriging standard deviation, an analogy to the statistical standard deviation, is provided.

3. MLD Criterion

3.1. Defining the Mixed Layer

[14] Our method of MLD climatology computation is based on direct MLD estimates from individual profiles with data at observed levels. These levels correspond to the vertical resolution of the probes. The average vertical resolutions of the profiles used to estimate the MLD are 8.2 m, 2.3 m, 19.5 m, and 9.4 m for PFL, CTD, XBT, and MBT observations, respectively. This is a different approach from the one based on already averaged profiles (KRH03, ML97), as these are altered by optimal interpolation and may have misleading information such as artificial density inversions or false vertical gradients, especially in sparse data areas (KRH03).

[15] In this paper, we define the MLD using the threshold method with a finite difference criterion. This method has been shown to better approximate the "true" MLD [*Thomson and Fine*, 2003] as compared to integral and regression methods. As shown in an experimental study by *Brainerd and Gregg* [1995], the MLD based on a difference criterion is also more stable than the MLD based on a gradient criterion, which requires sharp gradient-resolved profiles. For each profile, successively deeper observed levels are examined until one is found with a parameter value (temperature, salinity, density) differing from the near-surface reference level value by more than the chosen threshold value. For temperature, an absolute difference was applied, marking any temperature increase or decrease greater than the threshold as the end of the mixed layer. Such cases of temperature inversions are known to occur at the base of barrier layers and in polar regions. A linear interpolation between observed levels [*Suga et al.*, 2004] is then used to estimate the exact depth at which the difference criterion is reached. This method requires a careful choice of the parameter and value, as the resulting MLD strongly depends on it.

[16] The density depends on both temperature and salinity and therefore can be a good parameter in estimating the vertically homogeneous mixed layer. However, density can exhibit cases of vertical compensation (section 4.3.2), and
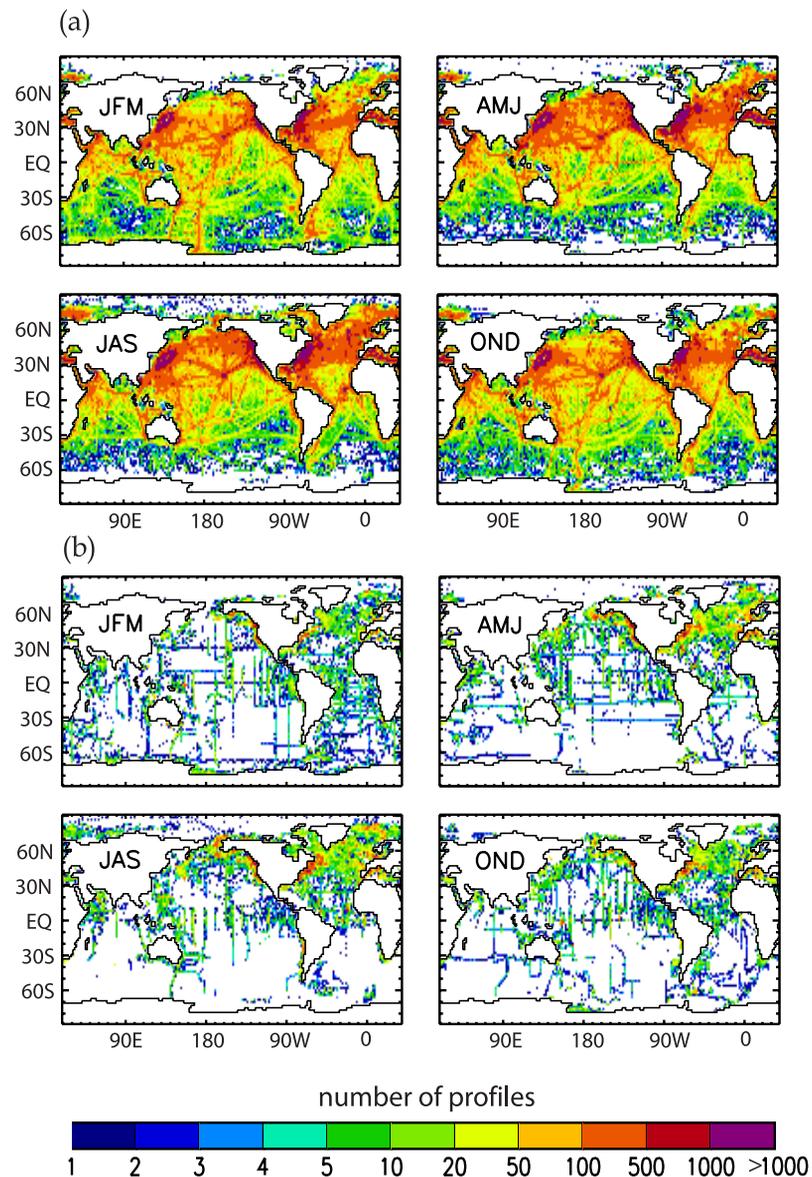
Figure 1. Number of (a) temperature profiles and (b) temperature-salinity profiles, in each 2° by 2° mesh box, from the NODC and WOCE databases. JFM, AMJ, JAS, and OND are the four seasons, respectively, January-February-March, April-May-June, July-August-September, and October-November-December. This also gives a confidence index for the field of MLD computed from those data.

above all, suffers from large geographical data holes (Figure 1). Temperature is then a possible alternative in estimating the MLD [e.g., *Rao et al.*, 1989], as it has a nearly complete seasonal coverage in the world ocean, including even the Southern Ocean, due to profiling floats released in this region starting in the 1990s. The resulting MLD will be far more reliable, though possible biases must be considered, particularly in barrier layer regions [*Lukas and Lindstrom*, 1991] (also see section 4.3.1), where salinity is the relevant parameter in determining the MLD, or in high-latitude regions where salinity is the major contributor to the density gradient. A correction for the pressure effect is applied by using the potential temperature and the potential density to estimate MLDs. As salinity has a weak effect on potential temperature, the computation is made with a constant ocean average salinity ($S = 34.72654$ PSU).

[17] The depth of the surface layer that is instantaneously mixed varies on many different timescales, from turbulence timescales to interannual variability, and a definition of the mixed layer implies a choice of timescale. The upper part of the ocean above the main thermocline encompasses the upper seasonal mixed layer, which is divided into an actively mixing layer and a daily remnant layer, and the underlying waters that have been in contact with the atmosphere within the last days, weeks, or months, for example, a fossil layer [*Sprintall and Roemmich*, 1999]. The mixing layer has a greater vertical uniformity than the mixed layer, and the maximum depth it reaches over a timescale on the order of a daily cycle or more defines the seasonal mixed layer [*Brainerd and Gregg*, 1995]. This is a useful descriptive schematic, but it strongly depends on the quantitative
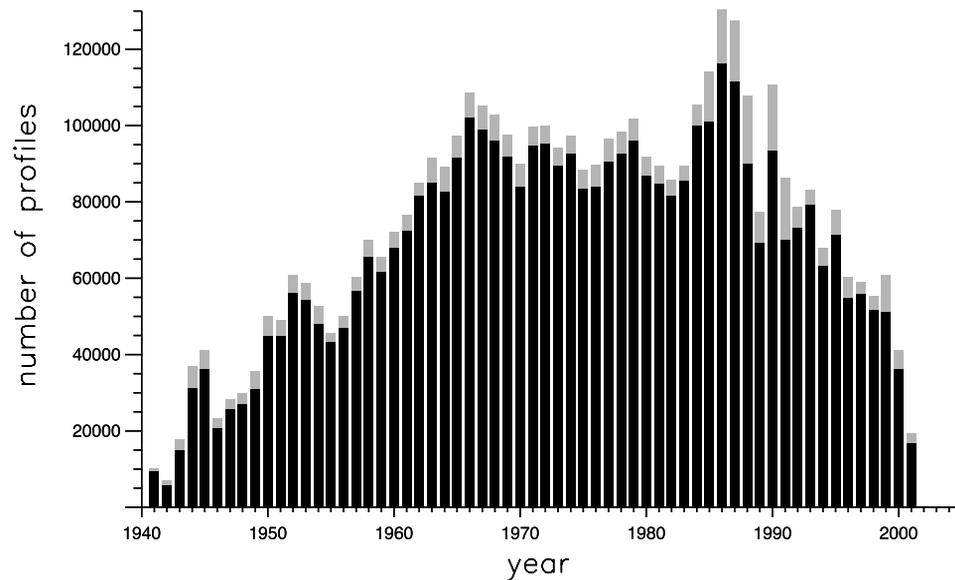
Figure 2. Temporal distribution of all profiles from the NODC and WOCE databases. Shading denotes total profiles (4,490,571 profiles), and black denotes temperature profiles selected after quality control (4,134,658 profiles). MBT profiles represent the majority of the data, with 52.9% of the total profiles. Since the mid-1960s, MBTs have been gradually replaced by XBT profiles, which are 38.8% of the data. The more recent CTDs and PFLs represent, respectively, 7.0% and 1.3% of the data set.

criteria which define the different layers. In our case, the MLD we want to estimate is the depth through which surface fluxes have been recently mixed and so integrated, recently meaning a timescale of at minimum a daily cycle, and no more than a few daily cycles. We must therefore avoid the diurnal variability of the mixing layer in our estimation while keeping the longer-term variability of the mixed layer. When the diurnal mixing layer occurs, it appears close to the surface. Measurements also often have some noise in the first few meters as instruments are introduced to the water, an additional practical reason for which we avoid the diurnal variability and the layer close to the surface.

3.2. Choosing a Threshold Value

[18] When estimating the MLD from an instantaneous profile, we must therefore take care to choose criterion values (i.e., the threshold value and reference depth) in agreement with the above description of the MLD. The choice of the appropriate value can have a strong influence on studies of mixed layer heat or salinity budgets which are highly dependent on the MLD [e.g., *Foltz et al.*, 2003].
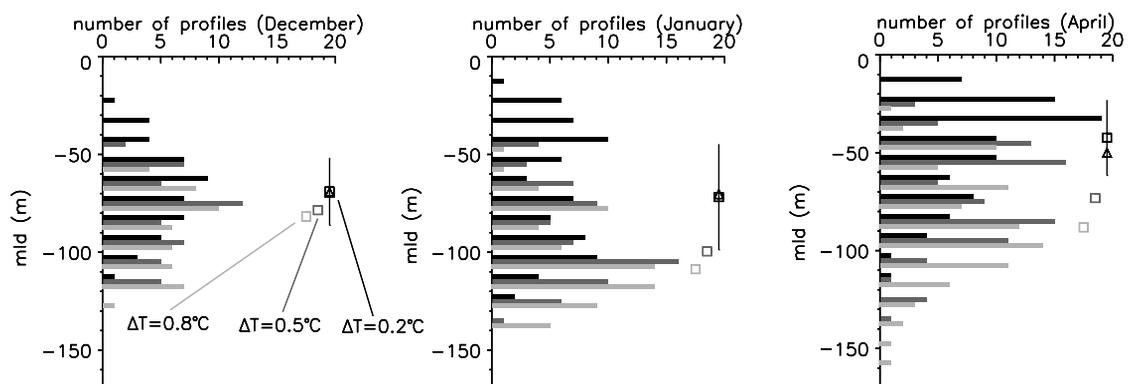

Figure 3. Distribution of MLDs in a 2° by 2° mesh box, located in the subtropical North Pacific (158°W, 26°N) for the months of December (48 profiles), January (68 profiles), and April (87 profiles), during winter and at the end of spring restratification. The three MLD criteria are $\Delta T = 0.2°C$ (black), 0.5°C (dark shading), and 0.8°C (light shading), from 10 m reference depth. Also indicated is the median for each criterion (squares) and the median average deviation (vertical bars) and mean (triangles) for the $\Delta T = 0.2°C$ criterion. Note the different distribution shapes for the 0.2°C criterion, successively Gaussian, bimodal, and skewed toward high values.

[19] The reference depth is therefore chosen to avoid the diurnal cycle of the mixing layer. A density threshold of 0.03 kg m^{-3} with a reference depth of 2.5 m was found to yield the mixing layer in equatorial regions, where the diurnal cycle is strong [*Schneider and Müller*, 1990]. During light winds and solar warming, temperature variations can reach 1 or 2°C in SST within the first 1−2 m [*Price et al.*, 1986]. Our reference depth is therefore set at 10 m to avoid a large part of the strong diurnal cycle in the top few meters of the ocean.

[20] The choice of the value of the threshold criterion in temperature and density was first based on visual inspection of a representative sample of randomly picked profiles, with a global spatial coverage and from all seasons. For each profile, MLDs based on a range of different temperature and density criteria were computed. Analysis of these profiles shows that the often standard 0.01 kg m^{-3} threshold yields too shallow a mixed layer for our purposes, often representing the mixing layer in profiles taken during the afternoon in temperate or tropical latitudes, which may have been preceded by strong solar heating. *Brainerd and Gregg* [1995] found that this threshold was in fact an upper bound in correctly determining the mixing layer rather than the mixed layer. A value of 0.1 kg m^{-3} sometimes yielded the depth of the main thermocline, in the case of fossil layers for example, and a value of 0.05 kg m^{-3} often falls within the seasonal thermocline rather than at its top. Therefore a threshold of 0.03 kg m^{-3} emerged as the appropriate value for the density criterion.

[21] A similar analysis for temperature returned a value between 0.1 and 0.2°C. We used 0.2°C, as 0.1°C occasionally returned the mixing layer depth. In addition, in high-latitude regions (surface temperatures of 4°C or less), a difference of 0.1°C corresponds to a too narrow density criterion of less than 0.01 kg m^{-3}. Finally, we used many MBT profiles, and their accuracy is often of 0.1°C, requiring a criterion of at least 0.2°C. The results given a posteriori in the MLD climatology using this criterion are indeed comparable with what can be seen in profiles shown by *Sprintall and Roemmich* [1999], for example. In their Figure 7, they show cases of fossil layers with the mixed layer between 70 and 120 m, while in the same region in June we find a monthly MLD of about 85 m with a median deviation of 30 m.

[22] The choice of MLD temperature criterion, in particular with respect to the choices of *Kara et al.* [2000b] and the classical 0.5°C threshold value from *Levitus* [1982], is further verified in comparison with several moored time series. Their high time resolution at a fixed point contrasts with the climatology's high number of profiles distributed widely in time. These comparisons show that the 0.2°C threshold criterion calculated from the 10 m temperature is fairly successful at estimating the MLD, and is particularly good at capturing the first springtime restratification. We used moored temperature data with high vertical resolution from several sources and different oceanic regimes, three of which are shown here. These are from the central Arabian Sea [*Weller et al.*, 2002], and the subtropical and subpolar gyres in the North Pacific (National Oceanographic Partnership Program).

[23] An estimate of the mixing layer depth was made using a threshold criterion of 0.1°C from the temperature closest to the surface. The criterion applied in our temperature-based climatology, a 0.2°C threshold difference from 10 m, was calculated, along with similar 0.5 and 0.8°C MLDs. These estimates of the MLD for the Arabian Sea are shown in Figure 4a. Toward the end of the winter monsoon, in February and March, the diurnal cycle in the mixing layer depth is particularly marked, and the 0.2°C MLD follows the several-day timescale envelope of the mixing layer depth quite well. The 0.5 and 0.8°C MLDs are similar in depth to the 0.2°C MLD during periods of mixed layer deepening, but during the spring restratification and to a lesser extent in the second fall restratification that occurs in the Arabian Sea, these criteria are not sensitive enough to capture the surface restratification, and result in a delayed shoaling of the mixed layer.

[24] A reduction of the time series data to monthly median values, the procedure used in creating the climatology (section 2.2), reveals that the 0.2°C MLD criterion remains a good estimator of the envelope of the mixing layer depth. The median of the minimum and maximum daily values of the mixing layer depth for the three time series locations are shown in Figures 4b−4d. The daily maximum MLD reflects the mixing layer depth on the daily timescale. During the summer monsoon in the Arabian Sea data, the mixed layer is maintained by wind forcing with no diurnal cycle (months of June and July in Figure 4a). However, a difference of about 10 m in the minimum and maximum median mixing layer depth is observed, as an oscillation of the base of the mixed layer, possibly created by internal wave variability. For the three sets of time series data, the 0.2°C MLD (red lines) are generally good at following the base of the mixing layer, and in the tropical and subtropical case, the major bias of the 0.5 and 0.8°C MLDs is a lag of 1−2 months in the spring restratification. In the subpolar gyre (Figure 4d), where wintertime surface temperatures descend to nearly 5°C, the 0.5 and 0.8°C criteria largely overestimate MLD, since the vertical temperature stratification is quite weak, and in fact the MLD is determined largely by the halocline (see section 4.3.1).

[25] To further investigate the spring restratification, we show the MLD distributions in a particular grid box for three representative months (Figure 3). The January bimodal distribution of the 0.2°C MLDs reflects the intraseasonal and interannual variability of MLDs at a time when first restratifications are already occurring. This shows that the 0.2°C criterion is more sensitive than the other two, and is also sensitive to the interannual and intraseasonal variability of the MLD.

4. Global MLD Distributions
4.1. Overview of the Temperature-Based MLD

[26] Monthly MLD distributions on a 2° grid, for the optimal $\Delta T = 0.2$°C temperature criterion, are shown in Figure 5. The seasonal distribution of the number of profiles used for each grid box (Figure 1a), also available on a monthly timescale, gives us a confidence index for the resulting MLD. Areas with less than three profiles per grid box should be considered more carefully than others.

[27] As spatial coverage of subsurface temperature data is fairly complete, the normalized kriging standard deviation
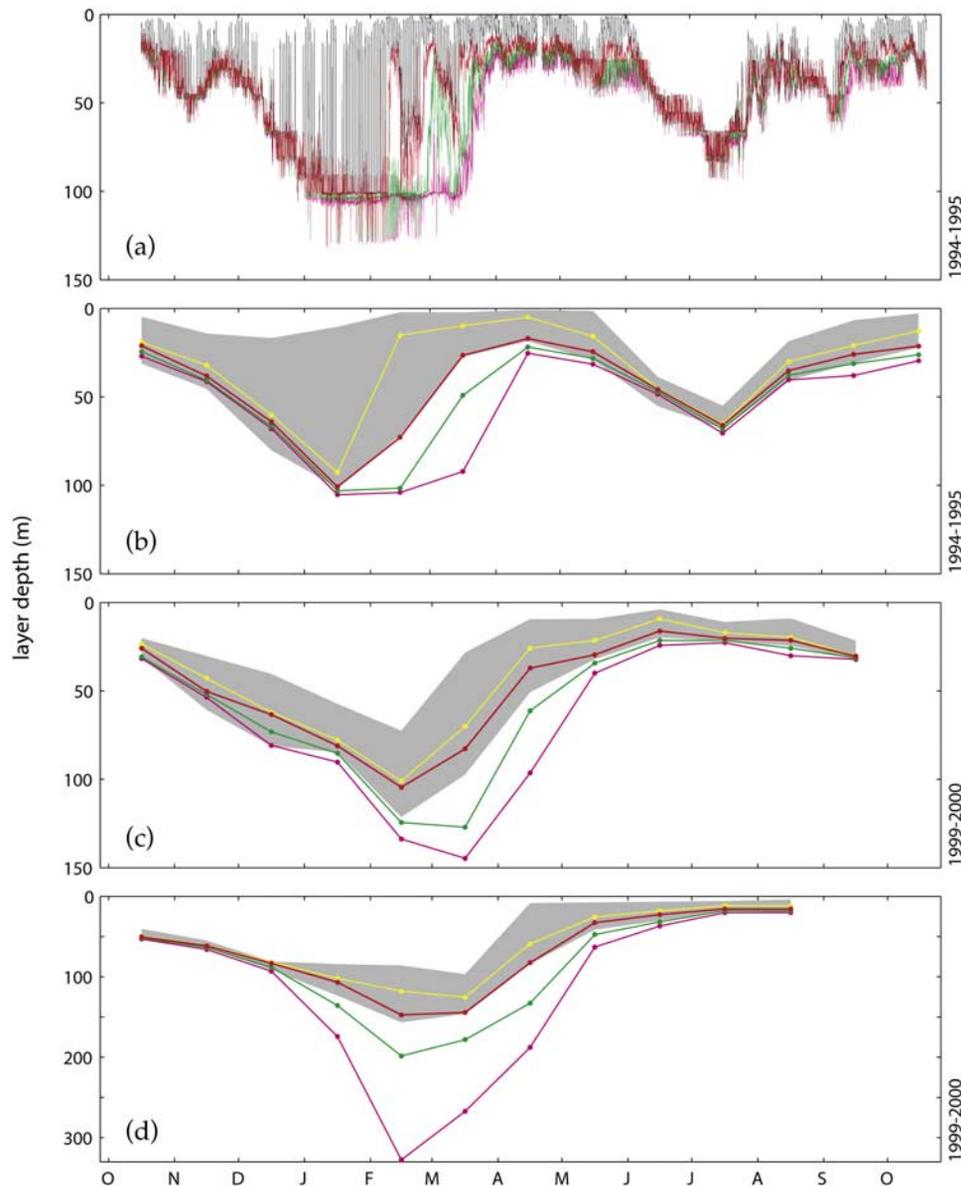
Figure 4. (a) A time series estimate of the mixing layer depth (black) from a mooring in the central Arabian Sea (61.5°E, 15.5°N), and the MLD calculated using three different threshold temperature criterion from the 10-m temperature: 0.2°C (red), 0.5°C (green), and 0.8°C (pink). (b) The monthly median values of the daily minimum and maximum mixing layer depth (shading), the instantaneous mixing layer depth (yellow), and the instantaneous MLD calculated using the same three criteria (and same colors) for the mooring in Figure 4a. (c) Same as Figure 4b, but for a mooring in the subtropical North Pacific (165°W, 35°N). (d) Same as Figure 4b, but for the subpolar North Pacific (145°W, 50°N).

of this MLD field is zero nearly everywhere (meaning no interpolation was applied), except in polar regions south of 55°S and in the Arctic Ocean. In these regions the kriging standard deviation increases up to about 0.3 and even locally to 0.8 in the wintertime southern Atlantic Ocean. The median absolute deviation, for each grid box not interpolated, is less than 20 m during summer and the beginning of autumn (June to October in Northern Hemisphere). It is less than 10 m in summer. It is 40 m on average (with maxima over 100 m in North Atlantic) in winter, a consequence of the large MLD variability at that time of year.

[28] The MLD climatology of Figure 5 presents many well-known features, which we briefly describe before a more detailed comparison with other methods and climatologies. There is a strong seasonal cycle in the subtropics and in midlatitudes, ranging from 20 m in summer to 150 m in winter. The MLD maxima are found in the wintertime North Atlantic deep water formation regions, with values around 740 m in the Greenland-Iceland-Norway (GIN) Sea and 550 m in the Labrador Sea. These mixed layers will be further discussed in section 5.1. The annual MLD is therefore more than 100 m in these regions, while in midlatitudes it is closer to 70 m.
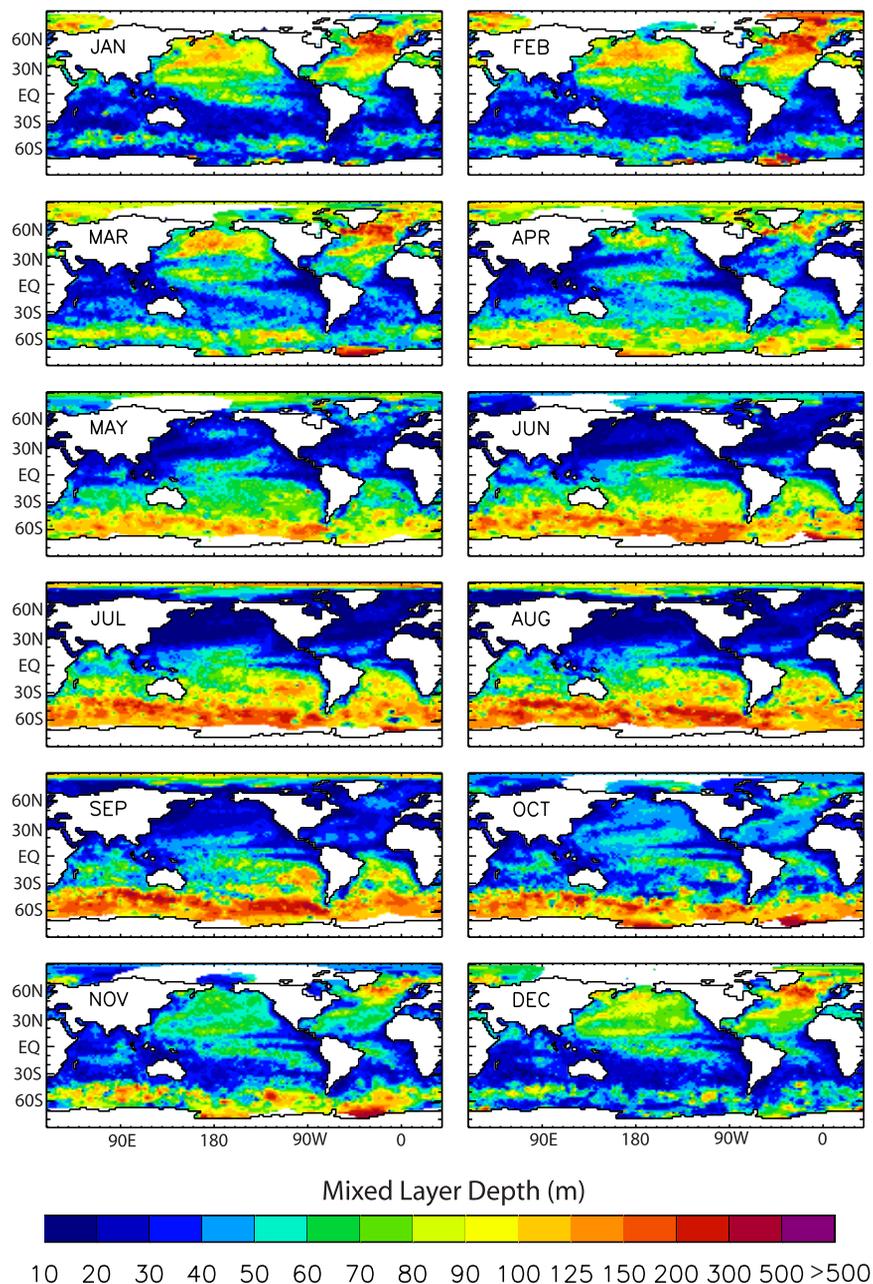
Figure 5. Mixed layer depth (MLD) climatology estimated from individual profiles, with an optimal temperature difference criterion of $\Delta T = 0.2°C$ from temperature at 10 m depth. Criterion was chosen from direct visual inspection of profiles and time series data. Data reduction was performed by taking the median of the MLDs on each 2° grid box followed by a slight smoothing and an optimal prediction method (ordinary Kriging) of missing data in a neighboring radius of 1000 km.

[29] In the northern Indian Ocean the semiannual cycle linked with monsoonal variability is well captured [*Weller et al.*, 2002]. The summer maps show a temperature-based MLD of about 50 m in the western equatorial Pacific; however, this is a region of known barrier layer formation [*Lukas and Lindstrom*, 1991], and will be further discussed in section 4.3.1. The Southern Ocean, between 45°S and 60°S, has a seasonal cycle with very deep MLDs in winter, reaching more than 300 m, and a deep minimum summer MLD of 70 m [*Rintoul and Trull*, 2001]. This seasonal cycle

is weaker south of 60°S, from 30 m in summer to values near 100 m in winter.

4.2. Methodology Comparison

[30] In this section, we isolate and evaluate the nonlinearity of the MLD computation on individual or on averaged profiles within a monthly grid box. We first calculated the monthly-averaged temperature profile for each box and at each fixed depth level as defined for the Levitus data (10, 20, 30, 50, 75, 100, 125, 150 m, every 50 m to 300 m, and
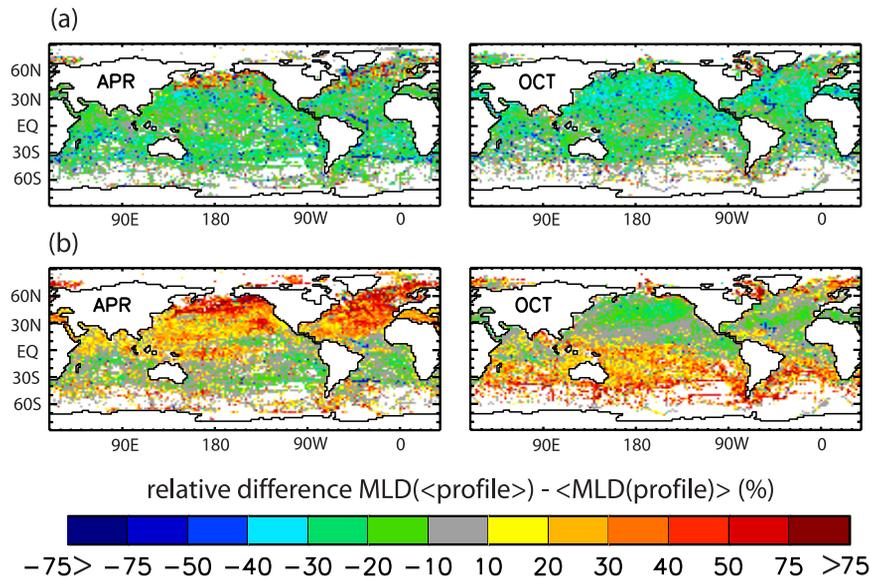
Figure 6. Relative difference between MLD estimated from the average profile, and average of MLDs estimated from individual profiles (a) using the same criterion $\Delta T = 0.2°C$ for both computations and (b) using $\Delta T = 0.5°C$ to estimate MLD from the averaged profile, and $\Delta T = 0.2°C$ for individual ones.

then every 100 m to a depth of 1000 m). We then compared the MLD estimated for this averaged profile with the average of the MLDs estimated from individuals profiles, using the same $\Delta T = 0.2°C$ criterion.

[31] The MLDs revealed by the averaged-profile climatology are globally 25% shallower than in the climatology based on individual profiles (Figure 6a presents the relative difference between the two for April and October). This can be understood by looking at the profiles in one individual grid box (Figure 7a). Averaging the individual profiles includes in the resulting averaged profile all gradients that have historically occurred in the month.

In Figure 7a there are eight profiles with gradients ranging from 0.2°C to 1°C between 10 and 50 m. Incorporating these profiles into the averaged profile yields an averaged stratification which is sufficient to be detected by the $\Delta T = 0.2°C$ criterion at around 50 m, while the averaged MLD only occurs at around 80 m. A sketch in Figure 7b also illustrates this phenomenon for a simple case with three profiles, one with a strong stratification near the surface. The global underestimation of the seasonal MLD by 25% using the averaged-profile method might be the reason why the 0.5°C criterion was chosen by ML97, or 0.8°C by *Kara et al.* [2000b].
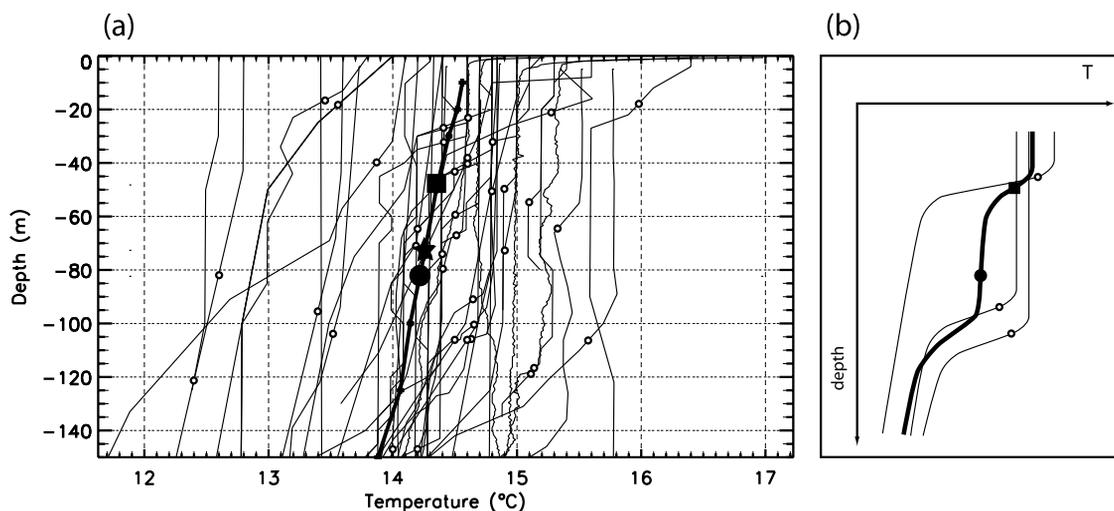

Figure 7. (a) Ensemble of 45 profiles contained in a mesh box in North Atlantic (20°W, 40°N), for month of March. The thick profile is the averaged one. Each open circle gives the MLD of the individual profiles, the solid square is the MLD for the averaged profile, the solid circle is the average of all MLDs, and the solid star is the median of those. (b) A sketch illustrating the same as in Figure 7a, but for a simple case of three profiles.
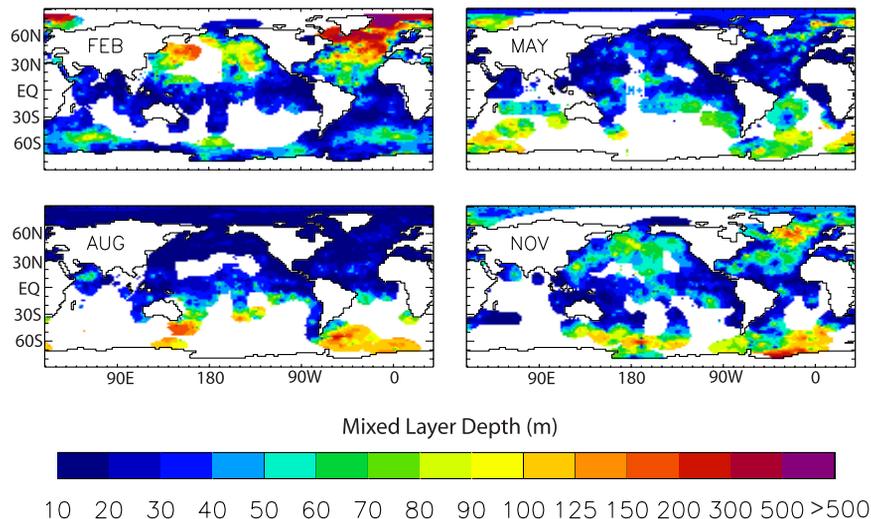
Figure 8. Same as for Figure 5, but for a density criterion of $\Delta\sigma_\theta = 0.03$ kg m^{-3}.

[32] The averaged-profile MLD climatology using a $\Delta T = 0.5°$C criterion and our individual-profile MLD climatology with the optimal $\Delta T = 0.2°$C criterion (Figure 6b) have more comparable MLD values, explaining why artificially higher values of the ΔT criterion are chosen for averaged-profile MLD climatologies. During the deepening of the mixed layer in autumn, some profiles may retain strong near-surface stratifications, leading to a shallower averaged-profile MLD climatology. On the other hand, in spring the averaged-profile MLD climatology is deeper, suggesting that the beginning of the restratification is not captured, as seen in section 3.2. This also suggests that MLD climatologies based on individual profiles but using a large criterion such as $\Delta T = 0.5°$C or $\Delta\sigma_\theta = 0.125$ kg m^{-3} might result in an overestimation of the MLD [e.g., *Suga et al.*, 2004] (or Pacific Fisheries Environmental Laboratory climatologies available online).

[33] Our method also avoids known problems such as averaging profiles from instruments with different maximum depths, which can lead to false vertical gradients, or density inversions due to interpolation over isobaric surfaces [*Lozier et al.*, 1994]. MLD climatologies based on the Levitus World Ocean Atlas may also have uniformly smoothed but coarsely resolved property fields, as the smallest radius of influence in the smoothing is 771 km [*Levitus*, 1982]. The benefit of our method is that we retain more detailed structures, as we do not spatially interpolate the temperature and salinity data. The strong signature of the Azores Current in winter is an example of the well-resolved structures in our climatology (January and February near 34°N in the eastern Atlantic Ocean in Figure 5).

4.3. Density-Based MLD: Barrier Layers and Salinity Compensation

[34] Although a temperature-based climatology of MLD works well in many locations, density remains a priori the most relevant parameter for creating a MLD climatology (see section 3). Figure 8 presents the density-based MLD climatology, using the optimal $\Delta\sigma_\theta = 0.03$ kg m^{-3} potential density criterion. The local kriging leaves blank regions where a reasonable interpolation was not possible due to the

sparsity of salinity data. The seasonal confidence index for this climatology, shown in Figure 1b, is less than 10, except in the North Atlantic where the normalized kriging standard deviation is zero from May to November and less than 0.4 for the rest of the year. Deep convection events in the winter GIN and Labrador Seas are present, with much deeper MLDs (over 1000 m) than in the temperature-based climatology. This difference, although also originating from the two different data sets used (see section 5.1), may be basically due to one of two effects. The first is that the thermal expansion coefficient of water is small at low temperatures. So while at 9°C, a 0.03 kg m^{-3} difference corresponds to an equivalent difference of 0.2°C, at 0°C for seawater it corresponds to a difference of 0.6°C, which yields a much deeper MLD in high-latitude cold waters, compared with a temperature-based difference of 0.2°C.

[35] The role of the halocline is also very important, and to verify its impact, we must remove the influence of variations of the thermal expansion coefficient. To do so we compute the MLD differences between a $\Delta T = -0.2°$C criterion and a variable density criterion corresponding to the same ΔT [e.g., *Vialard and Delecluse*, 1998; *Sprintall and Tomczak*, 1992],

$$\Delta\sigma_\theta = \sigma_\theta(T_{10} + \Delta T, S_{10}, P_0) - \sigma_\theta(T_{10}, S_{10}, P_0)$$
$$\simeq \frac{\partial\sigma}{\partial T}(T_{10}, S_{10}, P_0) * \Delta T,$$

with T_{10}, S_{10} the temperature and salinity values at the reference depth ($Z_{ref} = 10$ m), and P_0 the pressure at the ocean surface to compute the surface potential density and remove the non-negligible effects of the compressibility of seawater [*Schneider and Müller*, 1990]. Any MLD difference between those two criteria will then only be due to salinity stratification, and this will give us the barrier layer thickness.

4.3.1. Barrier Layers

[36] The equatorial barrier layer (BL) regions are easily identified in the four seasonal maps of this difference in MLD (Figure 9), especially the large BL in the western
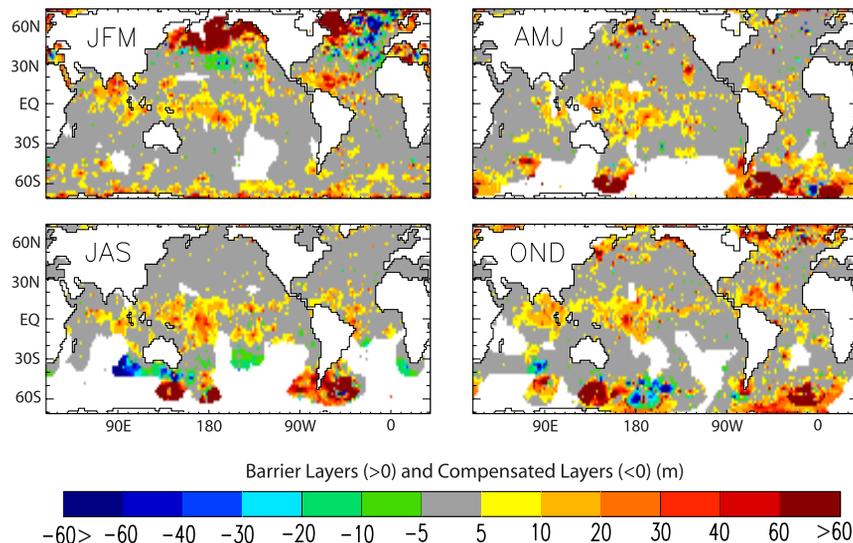
Figure 9. Seasonal maps of MLD difference between a $\Delta T = -0.2°C$ criterion and a variable $\Delta\sigma_\theta$ criterion corresponding to a fixed ΔT decrease of 0.2°C (after kriging).

equatorial Pacific Ocean during all seasons (between 15°S, 15°N and 150°E, 160°W). All the regions of the ITCZ (Intertropical Convergence Zone) and SPCZ (South Pacific Convergence Zone), where rainfall is more pronounced in the climatological mean, also have barrier layers [*Sprintall and Tomczak*, 1992]. The BL climatology shows a seasonality that has a tendency to follow the precipitation seasonal cycle, with the ITCZ BL being more pronounced in boreal summer and the SPCZ BL somewhat more pronounced in austral summer. The bias compared to the temperature-derived MLD is around 20 m in all seasons in these regions. A marked BL can be seen in the Bay of Bengal and eastern equatorial Indian Ocean beginning in boreal fall and developing in winter, reaching ∼40 m [*Masson et al.*, 2002; *Rao and Sivakumar*, 2003]. This BL is accompanied by a signal of about 20 m in the southeastern Arabian Sea during the same period [*Durand et al.*, 2004]. In the western tropical Atlantic Ocean a remarkable BL of more than 40 m develops in winter between 10°N and 20°N, where the evaporation minus precipitation budget is known to be positive. This BL must therefore originate in advective processes or continental runoff from the Amazon River [*Sprintall and Tomczak*, 1992].

[37] In winter at high latitudes, for example, the North Pacific or Labrador Sea, the MLD is also determined by the halocline [*Kara et al.*, 2000a]. These so-called BLs can reach more than 400 m in winter when the thermocline has disappeared in polar regions. This is due to local profiles which typically have temperature inversions at around 100 to 200 m depth and no decrease in temperature above. This yields a MLD of only 100 m in winter in the temperature-based climatology (Figure 5), and a difference with the equivalent density-based climatology which is only 20 to 30 m shallower (not shown). This suggests that the criterion used to identify barrier layer regions may not be relevant at high latitudes (poleward of 60° north or south), where it always returns large positive values (≃100 m or more).

4.3.2. Vertically Compensated Layers

[38] The difference between the temperature and density based MLDs has, in addition to barrier layers, significant regions where the density-based MLD is deeper than the temperature-based MLD (negative regions in Figure 9). They occur in the subtropical gyres and subtropical convergence zone in each winter hemisphere, and also at high latitudes in the wintertime North Atlantic Ocean. They correspond more generally to mean annual negative Ekman pumping regions. Similar compensations were noted by ML97 and KRH03 in the wintertime Northern Hemisphere subtropics, and by *Weller and Plueddemann* [1996] in the North Pacific.

[39] These regions correspond to profiles with an isothermal layer shallower than the isopycnal one, and thus where vertical compensation has occurred between salinity and temperature, creating a compensated layer (CL) beneath the well-mixed layer. Figure 10 shows two typical examples of such profiles. In such cases, active mixing cannot occur throughout the isopycnal layer if there are substantial temperature and salinity gradients within it.

[40] Such structures may be difficult to explain using one-dimensional surface-driven upper ocean physics, since it would require a well-compensated buoyancy flux. However, several mechanisms based on three-dimensional upper ocean physics are possible (Figure 11). Horizontal compensations within the mixed layer have been observed in the wintertime North Pacific subtropical gyre [*Rudnick and Ferrari*, 1999], near the subtropical front in the southeastern Indian Ocean [*James et al.*, 2002], and seem to be ubiquitous in deep (>75 m) mixed layers at horizontal scales smaller than 10 km [*Rudnick and Martin*, 2002]. The proposed mechanisms of the vertically compensated layer (Figure 11) are linked to these horizontal compensations.

[41] In the wintertime subtropics, the extent of the compensated layers may be simply due to the temperature-salinity relation of the water column linked to active subduction processes at midlatitudes. These processes would bring cold and fresh surface waters from higher latitudes to the upper thermocline directly beneath the profiled mixed layer. At lower latitudes, the warmer and saltier surface water of the mixed layer may have been horizontally-compensated with the subducted water, and
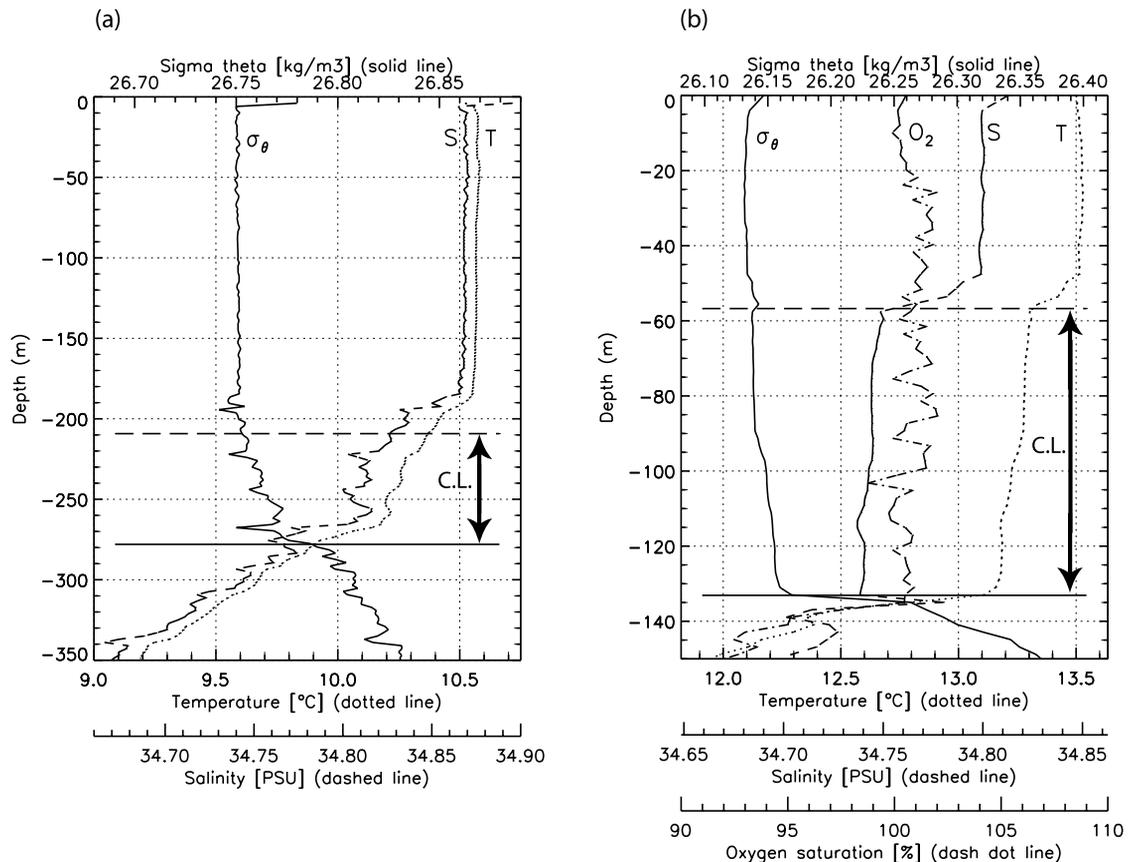
Figure 10. (a) Temperature, salinity, and density profile measured from CTD, on 17 July 1995, 0920 local time (LT), south of Australia (146.2°E, 44.4°S). (b) Temperature, salinity, density, and oxygen saturation profile measured from CTD, on 12 August 1991, 0530 LT in subtropical South Pacific (150.5°W, 37.0°S). These profiles show vertically compensated layers (C.L.) of about 70 m.

this would create a vertical compensation (Figure 10a). Such a mechanism has been further studied by *Sprintall and Tomczak* [1993], or *Tomczak and Godfrey* [1994], and would lead to an isopycnal layer including both the mixed layer and the upper thermocline. However, other structures of compensated layers such as in Figure 10b, with a thick homogeneous compensation layer below the surface mixed layer, may demand explanation by different physical processes.

[42] *Stommel and Fedorov* [1967] proposed an explanation based on lateral advection of horizontally compensated water masses, in which the Ekman drift of only an upper fraction of the mixed layer slides a different water mass over a lower one, leading to a vertical density compensation such as the one of Figure 10b. We also note the high level of oxygen saturation in the lower layer which may have been recently in contact with the atmosphere before the advection of the upper layer. Such an Ekman drift was also suggested by *Rintoul and Trull* [2001] as a plausible mechanism for vertical compensations found in winter near a strong horizontally density-compensated front south of Australia.

[43] One large region of compensated layers occurs in regions of deep convection in the wintertime GIN Seas (Figure 9). Slantwise convection [*Straneo et al.*, 2002], where active convection is tilted from the vertical due to rotational forces, might bring actively convecting, hori-

zontally surface-displaced, and potentially horizontally-compensated water underneath the surface waters at the profile location.

[44] Finally, the theoretical explanation for the observed horizontal compensations within the mixed layer relies on existing horizontal gradients in temperature and salinity, which then slump as density currents and are vertically mixed by surface forcing [*Ferrari and Young*, 1997]. Once created and during a break in vertical mixing, if the horizontal compensations are not perfect, they will slowly slump. This would create vertical compensations that are not exactly perfect (like the one in Figure 10b), but which may be missed by the MLD density criterion.

[45] When compensated layers exist, the temperature criterion gives the true MLD while the density criterion returns a layer where temperature and salinity are not vertically homogeneous, and hence a layer where a convective overturning does not occur. These are cases for which density is not the right parameter in selecting the thermodynamic MLD. Just as temperature is not appropriate in barrier layer regions, density is not in compensated layer regions.

4.3.3. An Optimal Estimate of MLD

[46] To deal with the previous result, the most reliable estimate of global MLDs might be a temperature-based climatology of MLD with its good spatial distribution,
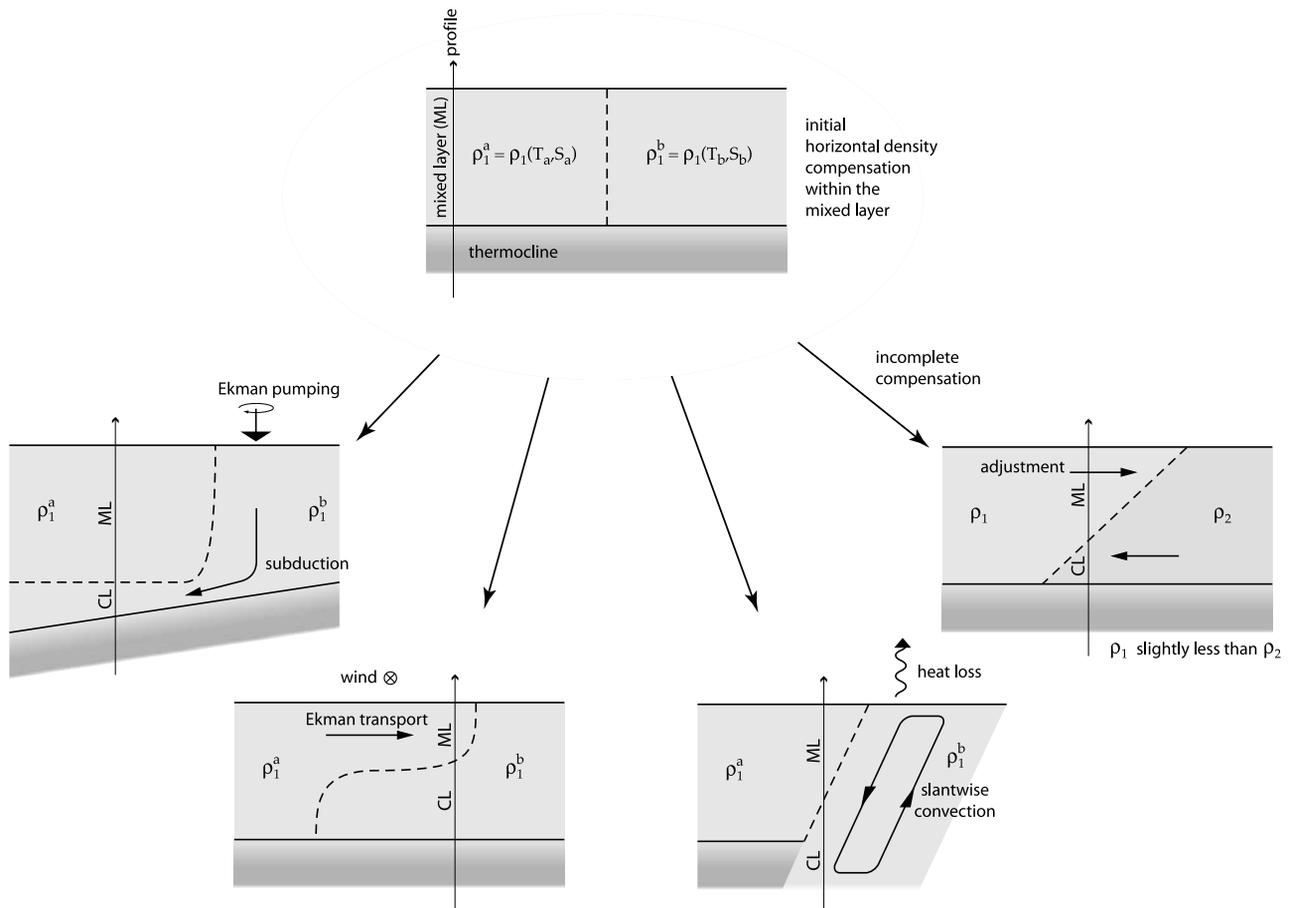
Figure 11. Schematics of the different three-dimensional mechanisms proposed to explain the occurrence of vertically compensated layer in the upper ocean.

augmented by an estimated correction in barrier layer regions. This could be more reliable than existing density-based climatologies, which have correct MLDs in barrier layer areas, but do not take into account compensated layers, and additionally have a poorer geographical coverage requiring large spatial and temporal interpolations.

[47] These MLD fields are produced by first estimating the fraction of barrier layer thickness relative to the MLD from the temperature-salinity data profiles. After spatial interpolation, a linear temporal interpolation between months gives better coverage to the correction. The resulting barrier layer fraction correction is finally applied to the temperature-based MLD field. This optimal estimate of the MLD will be further discussed in the following section.

5. Comparison With Other Estimates of MLD

[48] In this section we focus on comparisons of the timing and amplitude of the maximum MLD between various climatologies. The deepest extent of the winter mixed layer, also called the "bowl" [*Guilyardi et al.*, 2001], defines the boundary between the interior ocean and the surface ocean which is, at least once in a year, in direct contact with the atmosphere through vertical mixing. It represents the MLD on a yearly timescale. The ventilation of the thermocline and the volumes and characteristics of water masses formed at the surface

strongly depend on it, and eventually yield the large-scale distributions of properties in the interior ocean.

5.1. North Atlantic Comparison With Other Climatologies

[49] In comparing our climatology with the two available published global products, ML97 and KRH03, we concentrate on an analysis of the temperature-based MLD in the North Atlantic. Compared to the density-based product and to other regions, a greater amount of data is available, giving the highest confidence possible in the comparison. Since the temperature-based MLD is misleading in locations where a barrier layer occurs, the comparison is also made with our optimal estimate of the MLD, based both on temperature and salinity. Figures 12 and 13 show the timing and maximum value of MLD in the seasonal cycle for the four products. Note that even in the North Atlantic, some grid boxes must be left without value in the optimal MLD, due to a lack of salinity profiles. Since the seasonal cycle is difficult to define in the tropics, this region is not shown in Figure 12.

[50] On the basin scale, both our temperature-based and optimal MLDs are characterized by a beginning of restratification (Figure 12) in January/February, about 1 month earlier than ML93 and KRH03, and in contradiction with the commonly cited February/March time frame for restratification [e.g., *Stommel*, 1979; *Williams et*
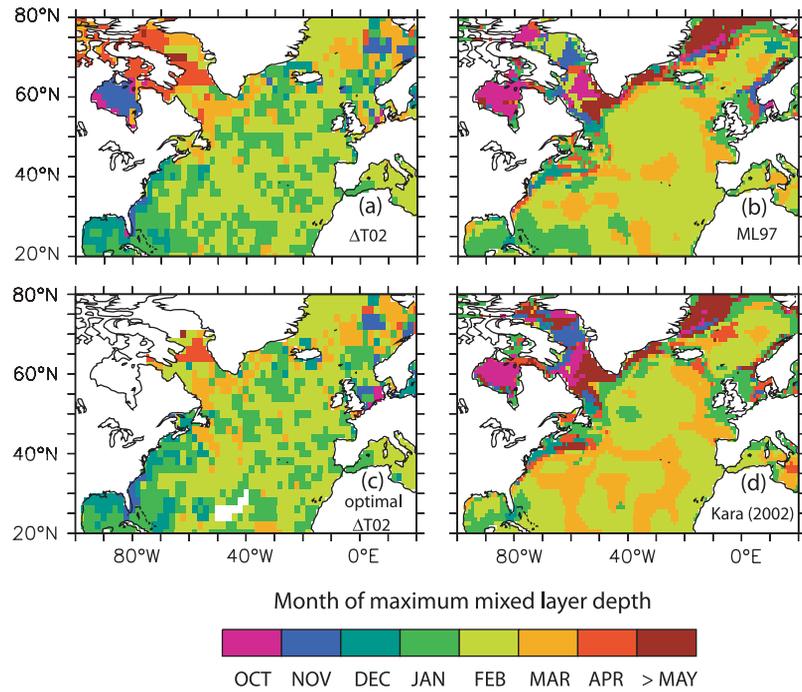
Figure 12. Month of maximum MLD reached in the North Atlantic for (a) the $\Delta T = 0.2°C$ climatology, (b) the *Monterey and Levitus* [1997] climatology ($\Delta T = 0.5°C$), (c) the $\Delta T = 0.2°C$ MLD climatology corrected in barrier layer regions, and (d) the *Kara et al.* [2002] climatology ($\Delta T = 0.8°C$).
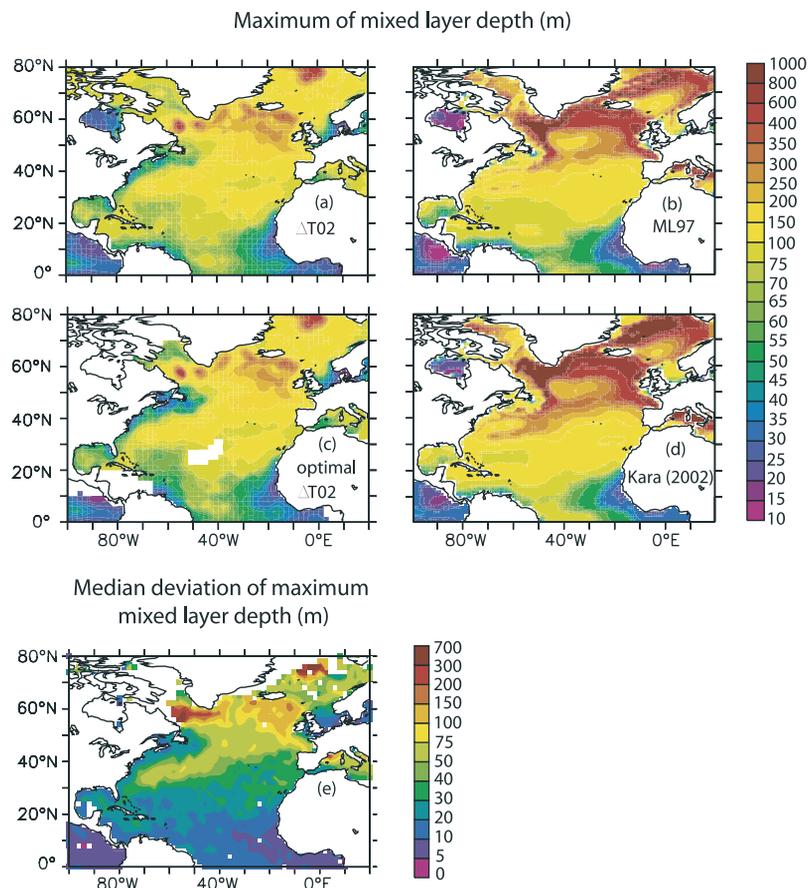

Figure 13. (a, b, c, d) Same as Figure 12, but for the maximum of MLD, and (e) the median deviation of the maximum MLD from the $\Delta T = 0.2°C$ climatology, estimated with at least four values per grid box.

al., 1995]. This difference in the timing of the maximum MLD likely originates in the choice of MLD criterion. As ML97 and KRH03 estimate the MLD from a temperature-salinity climatology, they use the larger criteria of 0.5°C or 0.8°C (section 4.2). In regions of weak surface stratification, such as the winter high latitudes, the larger criteria in fact measure changes deeper in the water column near the top of the thermocline, and are unable to detect weaker restratification events. This induces a delay in the timing of the seasonal MLD maximum, as seen in Figure 4. There are, however, modeling [*Lazar et al.*, 2002] and observational [*Takeuchi and Yasuda*, 2003] analyses that support the early restratification seen in our climatology.

[51] On smaller scales, other differences appear, especially in the Arctic seas (i.e., east of Greenland and in the Labrador Sea), where the deepest MLDs often appear much later in the year in ML97 and KRH03 as compared to the current climatology. Again, this is likely an artifact of the larger temperature criteria, which in polar regions marked by weak vertical temperature gradients are even more likely to pick out the main thermocline rather than changes in mixing. This is supported by the slight delay in KRH03 as compared with ML97 in these regions, corresponding to the larger criterion used. Between our temperature-based and optimal MLD, the small differences appear by construction in regions of barrier layers (see Figure 9, JFM) like the North Sea, around Newfoundland, and east of the Caribbean islands.

[52] As the climatologies represent a bulk monthly value of MLD, the actual timing of the peak MLD and therefore of the last ventilation with the atmosphere may be masked. If the daily maximum in MLD over the year occurs near the beginning of a month, and is followed by spring restratification events, the median MLD of this month may be smaller (though it will have greater variability) than the previous month. An example is seen in the time series shown in Figure 4a, where the maximum daily MLD (red curve) is reached at the beginning of February, while the maximum monthly median MLD is found in January. A better estimate where data are available would be to increase the time resolution of the climatology.

[53] A striking dynamical pattern evident from the maximum yearly MLDs (Figure 13) is the main deep convection sites in the Labrador and GIN Seas. The deep maxima (550 m in the Labrador Sea and 740 m in the GIN Sea) are more clearly identified in our climatology, and their depth, variability, and location are well placed [*Lavender et al.*, 2002]. They are also shallower than reported by MLD97 and KRH03, where the deep convection sites are found within larger areas of deep constant MLD of about 1000 m. Again, the difference in MLD criterion plays a role in the differences between climatologies. In the northern North Atlantic the $\Delta T = 0.2$°C climatology yields values of around 350 m with a median deviation between 100 m and 150 m, while ML97 and KRH03 reach values over 600 m. The larger temperature criteria in these latter two appears to be capturing deeper thermocline gradients instead of the base of the mixed layer, particularly in these low temperature stratification situations.

[54] The limitations of a climatology with its bulk time and space resolution in studying these episodic deep convection events are clear. Some complementary information

is found in the MLD median deviation (see Appendix A) shown in Figure 13e, representing the variability of the estimated MLD over the month. The sum of the MLD and median deviation, while not statistically rigorous, gives an order of magnitude for the maximum depth reached during the month, a quantity which may be more important for ventilation and water mass formation than the median MLD. The sums of the MLD and median deviation are 840 m for the Labrador Sea and 1200 m for the GIN Seas, in agreement with previous studies [*Lavender et al.*, 2002; *Schott et al.*, 1993]. MLDs from individual profiles using the $\Delta T = 0.2$°C criterion can be found greater than 1000 m in these regions, but in the same grid box one finds MLDs of 200 or 300 m. The small spatial scales and timescales of deep convective events make them hard to capture in a climatology; however, the same methodology has been applied at 0.5° resolution in the Mediterranean Sea, yielding well-known MLDs of around 1000 m in the Gulf of Lions (F. d'Ortenzio et al., On the Mediterranean mixed layer variability from a new climatology based on individual profiles, manuscript in preparation, 2004). The slight smoothing in our climatology compounds this limitation, reducing the MLD maximum in the Labrador Sea from 775 m to 550 m, for example. One final bias may come from shallow observations, particularly MBTs, which end before the base of the mixed layer in deep convection and deep MLD situations. This may introduce a shallow bias in our climatology of up to 50 m in winter in the northern North Atlantic.

[55] The shallow MLD maximum regions (less than 50 m) found along North America and northern Europe, within the Mediterranean Sea, and widespread in the tropics, are another important feature of this comparison. They correspond to major barrier layer regions (see Figure 9, JFM), and are major regions of difference between our climatologies and ML97 and KRH03. These differences are especially pronounced in the midlatitudes, with both ML97 and KRH03 missing the extended regions of shoaling observed toward the coasts. Within the tropics the three temperature-based products are fairly similar. Only the optimal MLD captures the coherent barrier layer signal centered at 60W between 10N and 30N, and the more tropical barrier layers. This optimal product, with its good estimate of MLD in both barrier layer and compensated layer regions, is the most reliable one, though it is somewhat hampered by the still-evident areas where the density-based correction cannot be calculated due to the sparsity of salinity data.

5.2. Global Comparisons With Oxygen MLD

[56] The 95% oxygen saturation limit from CTD data is a useful proxy in determining the maximum annual MLD [*Reid*, 1982]. It also provides another way to estimate wintertime MLD, especially in the Southern Ocean where temperature and salinity data are very sparse (Figure 1). For instance, oxygen saturation data have been used to estimate the convection depth in southeast Pacific Ocean [*Tsuchiya and Talley*, 1998]. Figure 14 presents the depth of the bowl estimated from both the oxygen saturation limit and the temperature-based climatology.

[57] Several regions of discrepancy of the estimates are found. The estimate of the bowl based on oxygen is shallower at high latitudes in the Southern Hemisphere, in the
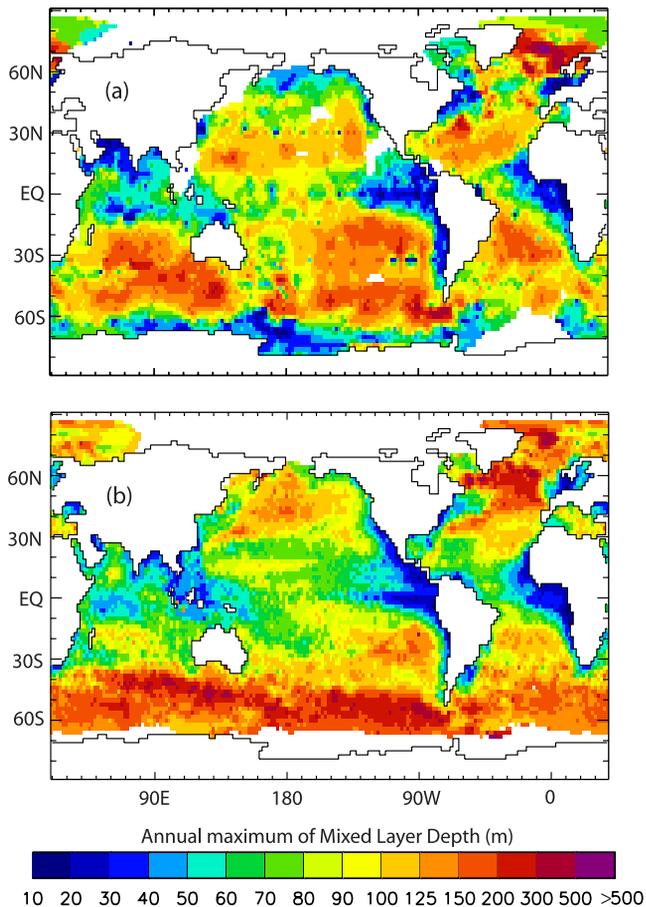
Figure 14. (a) Depth of the 95% oxygen saturation limit from CTD data, after kriging, giving a proxy for maximum winter MLD [*Reid*, 1982] also called "bowl" [*Guilyardi et al.*, 2001], and (b) maximum annual MLD from the $\Delta T = 0.2°C$ criterion climatology.

Antarctic divergence. Taking into account density-derived MLD (see Figures 8 and 9), we find that the influence of salinity in these regions cannot completely explain the observed discrepancy. Oxygen-based estimates from data collected during the austral summer could be biased because of the intense vertical movement of layers caused by the positive Ekman pumping. Other regions of discrepancy are the middle and high latitudes in the Northern Hemisphere, especially in the North Atlantic. In this regard, we note that the assumption of *Reid* [1982] is that 95% oxygen saturation corresponds to the oxygen dissolved during ventilation at the surface at the time of the deepest convective mixing during the year. The choice of the 95% threshold takes into account the moderate respiration occurring in the water column during the season. In areas where the export production is very high at specific times of the year (e.g., the North Atlantic spring bloom or the bloom in the Malvinas confluence), the oxidation of material exported from the surface respiration may consume enough oxygen to drive its concentration below the 95% value, thus altering the estimated maximum MLD. The oxygen-based estimate of the bowl is larger than the temperature-based one in all the subtropical gyres. One reason is the persistent downwelling Ekman

pumping. On the other hand, it is interesting to find a good correspondence in the southeastern corner of the Pacific, suggested formation region of Antarctic Intermediate Water (AAIW) [e.g., *Hanawa and Talley*, 2001].

6. Summary and Conclusions

[58] In a distinct departure from previous studies, a new climatology of the global ocean MLD has been built based on more than 4 million individual profiles selected after quality controls. This method retains more detailed structures in the resulting MLD fields, as no merging by smoothing or interpolating the profile data is necessary. This merging loses the information contained in individual profiles, and can also potentially yield artificial features.

[59] Careful consideration was taken to choose a MLD criterion that is instantaneously physically reliable. After a review of mixed layer processes, a visual inspection of a representative sample of profiles led to threshold values of 0.03 kg m^{-3} for density and $\pm 0.2°C$ for temperature, with a reference depth at 10 m. This criterion was further validated in comparisons to fixed time series data, and the resulting MLD best followed the base of the mixed layer, especially during restratification events at the end of winter. The principle is that the mixed layer as we defined it is the layer that has been actively mixed within the past day or few days, and since we are acting on individual profiles and taking a reference value below the bulk of the diurnal layer at 10 m, we want to take the smallest value possible. This value is mainly limited by the error in the data (MBT) at $0.2°C$.

[60] We investigated the consequences of the use of individual rather than averaged profiles in calculating the MLD. For a given criterion of $0.2°C$, the MLD estimated from averaged profiles has a global shallow bias of about 25% compared to estimates on individual profiles, within the same monthly grid box. However, MLDs are more comparable between the two methods if a $0.5°C$ criterion is used on the averaged profiles, explaining why this value is commonly used, even though it overestimates the MLD if used on individual profiles. The $0.5°C$ criterion is the best criterion for averaged profiles, but it is no more than a fit to the proper instantaneous calculation, and it introduces other biases.

[61] As salinity data are still too sparse, our global density-based MLD climatology computed from individual profiles has large regions with no value, especially in the Southern Ocean and the southern Atlantic, Pacific, and Indian oceans. Nevertheless, by restricting the computation to a seasonal climatology, a global estimation of barrier layers was created, and enabled us to point out regions where the salinity stratification controls the density stratification. It shows a prevalence of vertically compensated layers in the subtropical gyres and in the subtropical convergence zone in the winter hemisphere. These extended areas correspond to regions of recently reported horizontal compensations within the mixed layer. Dynamical oceanic processes, and especially subduction or Ekman advection, are proposed as possible explanations for this phenomenon. In such regions, the density criterion alone significantly overestimates the depth of the convective overturning, which physically defines the mixed layer, and the temper-

ature criterion is more representative. An optimal estimate of the MLD was then proposed, based on a temperature criterion offering the best spatial and temporal coverage, combined with a salinity criterion in barrier layer regions.

[62] Finally, intercomparisons using existing estimates of MLD from different climatologies and parameters were made. Within the North Atlantic in winter, the timing of the beginning of restratification was found to be about 1 month earlier (January/February) than in previous MLD climatologies (February/March). This is due to the fact that in high-latitude weak stratification conditions (such as those found in the wintertime Labrador and GIN seas), a too large temperature criterion detects deep thermocline movements instead of MLD variations. The maximal winter MLD presented here better identifies the deep water formation regions and is shallower than previously estimated. We may, however, underestimate deep winter MLDs as they are not reached by some instruments with limited depth range (MBTs, for example). Climatologies also represent the bulk monthly MLD over a grid box, making deep convection events with their limited time and spatial scales difficult to resolve. On the other hand, the larger criteria used in other climatologies, while making these zones more evident, lead to artificial structures with MLDs of 1000 m over a large part of the Labrador Sea in winter. This maximum annual MLD ("bowl") was also estimated from oxygen data and showed differences with the temperature bowl due to salinity effects, Ekman pumping, and biological activity impacts on oxygen.

[63] As the amount of data increases and by consequence the observed spatial and temporal resolutions of the subsurface ocean increase, the methodology presented here for estimating MLDs, with its sound physical basis, should be used instead of the one based on averaged profiles. Comparisons with ocean models should be made with MLDs that are computed at each time step and then averaged, yielding more consistent comparisons. This would also allow a choice of criterion to agree with those directly applied to the data profiles. A complete MLD climatology based on both temperature and salinity should become possible in the coming years as the Argo profiling float network grows. Our MLD climatology will be maintained and updated as the data available increase, and we intend it to be available for many uses, among them OGCM validation, biological studies, and mixed layer heat budget calculations. The climatology and associated quantities are available at http://www.lodyc.jussieu.fr/~cdblod/mld.html.

Appendix A: Methodology

A1. Selection of Profiles and Quality Control

[64] Since the goal of this work is to produce a MLD climatology based on individual profiles, our quality control method is designed to identify and eliminate any profile that is useless in the MLD computation, or erroneous, containing atypical data. As MLD is estimated for each profile, the first check is to keep only those profiles which allow us to compute a MLD. The surface reference depth chosen in this study for the MLD criterion is 10 m. We therefore only keep temperature profiles beginning above 10 m, and we consider the 6189 profiles starting between 10 and 12 m as if their first level was 10 m. This first step removes 79,540

profiles, 1.77% of the total. Most of them are XBTs, principally located in the area of Japan and in the North Pacific.

[65] We also have to deal with profiles ending before they reach the MLD criterion. They represent about 6% of the total, and are mostly located in the winter hemisphere where MLDs reach their maximum. Around 63% are MBTs, since they originally were shallower than today's standard (~300 m). These profiles provide us with a lower limit for the MLD, and simply ruling them out would introduce a shallow bias in the climatology [Polovina et al., 1995]. To partially overcome this problem, we keep the profiles ending deeper than the first estimated MLD of the associated grid box (about 3.3% of the total). We take the depth they reach as their estimated MLD, and the new estimate of MLD in the grid box will therefore include the maximum amount of information we can extract from the profiles.

[66] A correction is then applied on certain categories of XBT profiles to correct for a systematic error in their drop rate equation. The new drop rate follows [Hanawa et al., 1995].

[67] Some very general verifications are made to reject obviously wrong data. A few WOCE PFL stations, which have not yet gone through NODC/OCL quality control procedures, are removed because of bad locations or missing values in depth. We also reject some CTD profiles whose temperature is not reported and are therefore useless. Finally, sensors occasionally get stuck during a profile, and those whose in situ temperature is the same for 800 m or more are eliminated, avoiding artificial stratifications in potential temperature. These peculiar cases represent only 0.025% of the profiles (1146 profiles).

[68] A first quality control check of the data eliminates values that are outside of broad property ranges. These ranges (for temperature, salinity, and oxygen) were defined by the NODC Ocean Climate Laboratory's tables [Conkright et al., 2002].

[69] Data with inversions in depth, or obviously unrealistic ones in temperature (more than $0.3°C\ m^{-1}$, flags from Conkright et al. [2002]) are also rejected, as are those with excessive temperature gradients (more than $0.7°C\ m^{-1}$, flags from Conkright et al. [2002]). This last test enables us to remove a series of MBT profiles that introduced strong biases on particular cruise tracks, especially during winter between the Gibraltar Straights and the United States, or during March in the Indian Ocean along the 90°E transect. When diagnosing MLD using the density criterion, we also reject profiles with density inversions greater than $0.02\ kg\ m^{-3}$.

[70] Any profile with one of these spurious values (including missing ones) occurring before the computation of the specified MLD is eliminated. These quality controls remove a total of 154,146 profiles for the $\Delta T = 0.2°C$ criterion (3.43%). Most of these eliminations are from the excessive temperature gradient check, mainly in the first 50 m of the profile.

[71] Our quality control reduces the final number of stations by approximately 8% for our $\Delta T = 0.2°C$ criterion. The number of profiles that ended before the base of the mixed layer increases greatly between the $\Delta T = 0.2°C$ and a $\Delta T = 0.5°C$ criteria. Indeed the number of MBT profiles rejected because they end before the base of the mixed layer

nearly doubled, as the MLD estimated from this last criterion is much deeper than the MLD from the $\Delta T = 0.2°C$ criterion. Finally, the total number of temperature-salinity profiles used after these quality checks represents only 6.8% of temperature-only profiles, giving a good idea of the lack of data concerning subsurface salinity and hence density as compared to temperature.

A2. Data Reduction and Smoothing

[72] Each profile is processed as outlined above, and several MLDs can be estimated based on different values of the threshold criterion. The MLDs from each profile and for a given criterion are sorted into monthly boxes of $2°$ latitude by $2°$ longitude. This grid resolution can adequately accommodate the sparsity of data in some regions, but represents a trade off. Where data density allows, a finer resolution of $1°$ would better resolve smaller-scale features of regimes such as western boundary currents.

[73] To give a monthly MLD value for each grid box, we must then find the appropriate statistical estimator which best characterizes the information we are seeking. In our case, each grid box contains the interannual and intraseasonal variability, which often result in a great range of MLD values. Those values are limited to a minimum of 10 m, which is the reference depth. We can expect broad distributions with some "outlier" points with extreme values. This appears to be rather true for our $0.2°C$ temperature criterion. MLD distributions in grid boxes with sufficient data are then often skewed, showing a tail in the deepest values. This is especially true in the spring and summer when the mixed layer is shoaling, with the relative skewness of the distributions showing values around 5, indicating a highly skewed distribution. In such cases (see, for example, April in Figure 3 for the $\Delta T = 0.2°C$ criterion), the median of the MLDs for each grid box is a more robust estimator than the mean, and more representative of the climatological field. If the distribution is much more Gaussian, then the median will be a good estimator as well. The median deviation is defined as

$$\alpha_{dev} = \frac{1}{N_{profiles}} \sum_{i=1}^{N_{profiles}} |MLD_i - MLD_{median}|,$$

and gives us an estimator of the width of the distribution for each grid box containing at least three values.

[74] At this stage we have a MLD climatology as the median monthly values along with the number of profiles used for each grid box, but with regions with no data. To partially overcome the noisy nature of ship observations, we then applied a slight smoothing. It is based on a two-dimensional smoothing operator that uses 50% self-weight and 50% adjacent weight from the eight neighboring observation values. To this, we add a weight that depends on the number of ship observations, giving the following MLD value for the grid box i_0:

$$MLD_{i_0} = \frac{1}{\sum w_i} \sum_{i \ neighboring \ i_0} w_i * MLD_I,$$

where $w_{i0} = 8 * f_s(n_{i0})$, $w_{i \neq i_0} = f_s(n_i)$, $f_s(n) = 1 - e^{-\frac{n^2}{4n_0}}$, and $n_0 = 20$, n_i being the number of profiles in grid box i. This value of n_0 is chosen so as to have an almost 100% confidence level for grid boxes with 20 profiles or more, and less than 10% for the those with three profiles or less. Such a weighting scheme enhances the quality and continuity of the climatology compared to a simple linear average approach [*Terray*, 1994].

A3. Data Kriging

[75] To fill in grid points where no data were available, the method of ordinary kriging is applied. Kriging is a very often used optimal prediction method in spatial data analysis which has close links to objective analysis. It is based on statistical principles and on the assumption that the parameter being interpolated can be treated as a regionalized variable, which is true for the MLD. Ordinary kriging assumes that local means are not necessarily closely related to the population mean, and therefore uses only the sample in the local neighborhood of the estimation location. Kriging builds a weighted average of those neighboring data so as to minimize the estimation variance which can be expressed in terms of the model covariances of the data [*Wackernagel*, 1998].

[76] We used an exponential covariance function to fit the experimental variogram for each data location. Three parameters are required for the variogram model. The "practical range" is taken to be 1000 km. It represents the distance over which the covariance function has decreased by 95%. The "nugget" is set to zero, implying that there is no variance discontinuity at the known data value. Finally, the "sill" was chosen to be the average variance of the sample, as it is the covariance function value for a high level of data separation.

[77] The neighborhood extent is defined as a circle of the same radius as the practical range value, as locations beyond it are uncorrelated with the estimated location and have therefore no direct influence. A minimum of five data were required in the neighborhood of a point to make an estimation at that location. The advantages of this geostatistical approach to interpolation are that kriging is an exact interpolator, which does not change any known values, and that, as a statistical method, it provides an indication of the estimation error in the kriging standard deviation.

References

Brainerd, K. E., and M. C. Gregg (1995), Surface mixed and mixing layer depths, *Deep Sea Res., Part A*, 9, 1521–1543.

Chen, D., A. J. Busalacchi, and L. M. Rothstein (1994), The roles of vertical mixing, solar radiation, and wind stress in a model simulation

of the sea surface temperature seasonal cycle in the tropical Pacific Ocean, *J. Geophys. Res.*, 99, 20,345–20,359.

Conkright, M. E., et al. (2002), *World Ocean Database 2001*, vol. 1, *Introduction*, edited by S. Levitus, *NOAA Atlas NESDIS 42*, 167 pp., Natl. Oceanic and Atmos. Admin., Silver Spring, Md.

Durand, F., S. R. Shetye, J. Vialard, D. Shankar, S. S. C. Shenoi, C. Ethe, and G. Madec (2004), Impact of temperature inversions on SST evolution in the Southeastern Arabian Sea during the pre-summer monsoon season, *Geophys. Res. Lett.*, 31, L01305, doi:10.1029/2003GL018906.

Ferrari, R., and W. R. Young (1997), On the development of thermohaline correlations as a result of non linear diffusive parametrization, *J. Mar. Res.*, 55, 1069–1101.

Foltz, G. R., S. A. Grodsky, J. A. Carton, and M. J. McPhaden (2003), Seasonal mixed layer heat budget of the tropical Atlantic Ocean, *J. Geophys. Res.*, 108(C5), 3146, doi:10.1029/2002JC001584.

Guilyardi, E., G. Madec, and L. Terray (2001), The role of lateral ocean physics in the upper ocean thermal balance of a coupled ocean-atmosphere GCM, *Clim. Dyn.*, 17, 1423–1452.

Hanawa, K., and L. D. Talley (2001), Mode waters, in *Ocean Circulation and Climate: Observing and Modelling the Global Ocean*, edited by G. Siedler, J. Church, and J. Gould, pp. 373–386, Academic, San Diego, Calif.

Hanawa, K., P. Rual, R. Bailey, A. Sy, and M. Szabados (1995), A new depth-time equation for Sippican or TSK T-7, T-6 and T-4 expendable bathythermographs (XBT), *Deep Sea Res.*, 42, 1423–1452.

James, C., M. Tomczak, I. Helmond, and L. Pender (2002), Summer and winter surveys of the subtropical front of the southeastern Indian Ocean 1997–1998, *J. Mar. Syst.*, 37, 129–149.

Kara, A. B., P. A. Rochford, and H. E. Hurlburt (2000a), Mixed layer depth variability and barrier layer formation over the North Pacific Ocean, *J. Geophys. Res.*, 105, 16,783–16,801.

Kara, A. B., P. A. Rochford, and H. E. Hurlburt (2000b), An optimal definition for ocean mixed layer depth, *J. Geophys. Res.*, 105, 16,803–16,821.

Kara, A. B., P. A. Rochford, and H. E. Hurlburt (2002), Naval Research Laboratory Mixed Layer Depth (NMLD) Climatologies, *Rep. NRL/FR/7330–02-9995*, 26 pp., Naval Res. Lab., Washington, D. C.

Kara, A. B., P. A. Rochford, and H. E. Hurlburt (2003a), Mixed layer depth variability over the global ocean, *J. Geophys. Res.*, 108(C3), 3079, doi:10.1029/2000JC000736.

Kara, A. B., A. J. Wallcraft, and H. E. Hurlburt (2003b), Climatological SST and MLD predictions from a global layered ocean model with an embedded mixed layer, *J. Atmos. Oceanic Technol.*, 20, 1616–1632.

Lavender, K. L., R. E. Davis, and W. B. Owens (2002), Observations of open-ocean deep convection in the Labrador Sea from subsurface floats, *J. Phys. Oceanogr.*, 32, 511–526.

Lazar, A., T. Inui, P. Malanotte-Rizzoli, A. J. Busalacchi, L. Wang, and R. Murtugudde (2002), Seasonality of the ventilation of the tropical Atlantic thermocline in a ocean general circulation model, *J. Geophys. Res.*, 107(C8), 3104, doi:10.1029/2000JC000667.

Levitus, S. (1982), Climatological atlas of the world ocean, *NOAA Prof. Pap. 13*, 173 pp., U.S. Govt. Printing Off., Washington, D. C.

Longhurst, A. (1995), Seasonal cycles of pelagic production and consumption, *Prog. Oceanogr.*, 36, 77–167.

Lozier, M. S., M. S. McCartney, and W. B. Owens (1994), Anomalous anomalies in averaged hydrographic data, *J. Phys. Oceanogr.*, 24, 2624–2638.

Lukas, R., and E. Lindstrom (1991), The mixed layer of the western equatorial Pacific Ocean, *J. Geophys. Res.*, 96, 3343–3357.

Masson, S., P. Delecluse, J.-P. Boulanger, and C. Menkes (2002), A model study of the seasonal variability and formation mechanisms of the barrier layer in the equatorial Indian Ocean, *J. Geophys. Res.*, 107(C12), 8017, doi:10.1029/2001JC000832.

McCreary, J. P., K. E. Kohler, R. R. Hood, S. Smith, J. Kindle, A. S. Fischer, and R. A. Weller (2001), Influences of diurnal and intraseasonal forcing on mixed-layer and biological variability in the central Arabian Sea, *J. Geophys. Res.*, 106, 7139–7155.

Monterey, G., and S. Levitus (1997), *Seasonal Variability of Mixed Layer Depth for the World Ocean*, *NOAA Atlas NESDIS 14*, 100 pp., Natl. Oceanic and Atmos. Admin., Silver Spring, Md.

Morel, A., and J. M. Andre (1991), Pigment distribution and primary production in the western Mediterranean as derived and modeled from coastal zone color scanner observations, *J. Geophys. Res.*, 96, 12,685–12,698.

Noh, Y., C. J. Jang, T. Yamagata, P. C. Chu, and C.-H. Kim (2002), Simulation of more realistic upper-ocean processes from an OGCM with a new ocean mixed layer model, *J. Phys. Oceanogr.*, 32, 1284–1307.

Obata, A., J. Ishizaka, and M. Endoh (1996), Global verification of critical depth theory for phytoplankton bloom with climatological in situ temperature and satellite ocean color data, *J. Geophys. Res.*, 101, 20,657–20,667.

Pailler, K., B. Bourlès, and Y. Gouriou (1999), The barrier layer in the western tropical Atlantic Ocean, *Geophys. Res. Lett.*, 26, 2069–2072.

Polovina, J. J., G. T. Mitchum, and G. T. Evans (1995), Decadal and basin-scale variation in mixed layer depth and the impact on biological production in the central and North Pacific, 1960–88, *Deep Sea Res., Part I*, 42, 1701–1716.

Price, J. F., R. A. Weller, and R. Pinkel (1986), Diurnal cycling: Observations and models of the upper ocean response to diurnal heating, cooling, and wind mixing, *J. Geophys. Res.*, 91, 8411–8427.

Rao, R. R., and R. Sivakumar (2003), Seasonal variability of sea surface salinity and salt budget of the mixed layer of the north Indian Ocean, *J. Geophys. Res.*, 108(C1), 3009, doi:10.1029/2001JC000907.

Rao, R. R., R. L. Molinari, and J. F. Festa (1989), Evolution of the climatological near-surface thermal structure of the tropical Indian Ocean: 1. Description of mean monthly mixed layer depth, and sea surface temperature, surface current, and surface meteorological fields, *J. Geophys. Res.*, 94, 10,801–10,815.

Reid, J. L. (1982), On the use of dissolved oxygen concentration as an indicator of winter convection, *Naval Res. Rev.*, 34, 28–39.

Rintoul, S. R., and T. W. Trull (2001), Seasonal evolution of the mixed layer in the Subantarctic Zone south of Australia, *J. Geophys. Res.*, 106, 31,447–31,462.

Rudnick, D. L., and R. Ferrari (1999), Compensation of horizontal temperature and salinity gradients in the ocean mixed layer, *Science*, 283, 526–529.

Rudnick, D. L., and J. P. Martin (2002), On the horizontal density ratio in the upper ocean, *Dyn. Atmos. Oceans*, 36, 3–21.

Schneider, N., and P. Müller (1990), The meridional and seasonal structures of the mixed layer depth and its diurnal amplitude observed during the Hawaii-to-Tahiti shuttle experiment, *J. Phys. Oceanogr.*, 20, 1395–1404.

Schott, F., M. Visbeck, and J. Fischer (1993), Observations of vertical currents and convection in the central Greenland Sea during the winter of 1988–1989, *J. Geophys. Res.*, 98, 14,401–14,421.

Spall, M. A., R. A. Weller, and P. W. Furey (2000), Modeling the three-dimensional upper ocean heat budget and subduction rate during the Subduction Experiment, *J. Geophys. Res.*, 105, 26,151–26,166.

Sprintall, J., and M. J. McPhaden (1994), Surface layer variations observed in multiyear time series measurements from the western equatorial Pacific, *J. Geophys. Res.*, 99, 963–979.

Sprintall, J., and D. Roemmich (1999), Characterizing the structure of the surface layer in the Pacific Ocean, *J. Geophys. Res.*, 104, 23,297–23,311.

Sprintall, J., and M. Tomczak (1992), Evidence of the barrier layer in the surface layer of the tropics, *J. Geophys. Res.*, 97, 7305–7316.

Sprintall, J., and M. Tomczak (1993), On the formation of central water and thermocline ventilation in the Southern Hemisphere, *Deep Sea Res., Part I*, 40, 827–848.

Stommel, H. (1979), Determination of watermass properties of water pumped down from the Ekman layer to the geostrophic flow below, *Proc. Natl. Acad. Sci. U. S. A.*, 76, 3051–3055.

Stommel, H., and K. N. Fedorov (1967), Small scale structure in temperature and salinity near Timor and Mindanao, *Tellus*, 19, 306–325.

Straneo, F., M. Kawase, and S. C. Riser (2002), Idealized models of slantwise convection in a baroclinic flow, *J. Phys. Oceanogr.*, 32, 558–572.

Suga, T., K. Motoki, Y. Aoki, and A. M. Macdonald (2004), The North Pacific climatology of winter mixed layer and mode waters, *J. Phys. Oceanogr.*, 34, 3–22.

Takeuchi, E., and I. Yasuda (2003), Winter shoaling of oceanic surface mixed layer, *Geophys. Res. Lett.*, 30(22), 2152, doi:10.1029/2003GL018511.

Terray, P. (1994), An evaluation of climatological data in the Indian Ocean area, *J. Meteorol. Soc. Jpn.*, 72(3), 359–386.

Thompson, R. O. R. Y. (1976), Climatological numerical models of the surface mixed layer of the ocean, *J. Phys. Oceanogr.*, 6, 496–603.

Thomson, R. E., and I. V. Fine (2003), Estimating mixed layer depth from oceanic profile data, *J. Atmos. Oceanic Technol.*, 20(2), 319–329.

Tomczak, M., and J. S. Godfrey (1994), *Regional Oceanography: An Introduction*, Pergamon, New York.

Tsuchiya, M., and L. D. Talley (1998), A Pacific hydrographic section at 88°W: Water-property distribution, *J. Geophys. Res.*, 103, 12,899–12,918.

Vialard, J., and P. Delecluse (1998), An OGCM study for the TOGA decade: I. Role of salinity in the physics of the Western Pacific fresh pool, *J. Phys. Oceanogr.*, 28, 1071–1088.

Wackernagel, H. (1998), *Multivariate Geostatistics*, 2nd ed., 291 pp., Springer-Verlag, New York.

Weller, R. A., and A. J. Plueddemann (1996), Observations of the vertical structure of the oceanic boundary layer, *J. Geophys. Res.*, *101*, 8789–8806.

Weller, R. A., A. S. Fischer, D. L. Rudnick, C. C. Eriksen, T. D. Dickey, J. Marra, C. Fox, and R. Leben (2002), Moored observations of upper-ocean response to the monsoons in the Arabian Sea during 1994–1995, *Deep Sea Res., Part II*, *49*, 2195–2230.

Williams, R. G., M. A. Spall, and J. C. Marshall (1995), Does Stommel's mixed layer "Demon" work?, *J. Phys. Oceanogr.*, *25*, 3089–3102.

WOCE Data Products Committee (2002), WOCE Global Data, version 3.0, *Rep. 180/02*, WOCE Int. Project Off., Southampton, UK.

Zhang, R.-H., and S. E. Zebiak (2002), Effect of penetrating momentum flux over the surface boundary/mixed layer in a z-coordinate OGCM of the tropical Pacific, *J. Phys. Oceanogr.*, *32*, 3616–3637.

―――――――――――――

C. de Boyer Montégut, A. Lazar, and G. Madec, Laboratoire d'Océanographie Dynamique et de Climatologie, Université Pierre et Marie Curie, Tour 45-55, 4ième étage, boîte 100, 4, place Jussieu, F-75252 Paris Cedex 05, France. (cdblod@lodyc.jussieu.fr; alban.lazar@lodyc.jussieu.fr; gurvan.madec@lodyc.jussieu.fr)

A. S. Fischer, Intergovernmental Oceanographic Commission, UNESCO, 1 Rue Miollis, F-75732 Paris Cedex 15, France. (a.fischer@unesco.org)

D. Iudicone, Laboratory of Biological Oceanography, Stazione Zoologica Anton Dohrn, Villa Comunale, I-80121 Naples, Italy. (iudicone@szn.it)